https://doi.org/10.5194/egusphere-2025-4058
Preprint. Discussion started: 28 August 2025

Residential burning is a significant source of soluble iron to the ocean

Rui Li,[1,#,a] Haley E. Plaas,[2,#,b] Yifan Zhang,[1,3] Yizhu Chen,[1,3] Tianyu Zhang,[1,3] Yi Yang,[4] Sagar Rathod,[5] Guohua Zhang,[1] Xinming Wang,[1] Douglas S. Hamilton,[2,*] Mingjin Tang[1,6,*]

[1] State Key Laboratory Advanced Environmental Technology and Guangdong Key Laboratory of Environmental Protection and Resources Utilization, Guangzhou Institute of Geochemistry, Chinese Academy of Sciences, Guangzhou, China

[2] Marine, Earth, and Atmospheric Sciences, North Carolina State University, Raleigh, NC, USA

[3] College of Earth and Planetary Sciences, University of Chinese Academy of Sciences, Beijing, China

[4] Key Laboratory of Geographic Information Science of the Ministry of Education, School of Geographic Sciences, East China Normal University, Shanghai, China

[5] Department of Atmospheric, Oceanic, and Space Sciences, University of Wisconsin-Madison, Madison, WI, USA

[6] Institute of Surface-Earth System Science, School of Earth System Science, Tianjin University, Tianjin, China

[a] Current affiliation: School of Public Health, MOE Key Laboratory of Coal Environmental Pathogenicity and Prevention, Shanxi Medical University, Taiyuan, China

https://doi.org/10.5194/egusphere-2025-4058
Preprint. Discussion started: 28 August 2025

[b] Current affiliation: Columbia University, Center for Climate Systems Research, New York, NY 10025, USA; NASA Goddard Institute for Space Studies, New York, NY, USA

Correspondence:

Mingjin Tang (mingjintang@126.com)

Douglas S. Hamilton (dshamil3@ncsu.edu)

The two authors contributed equivalently to this work.

https://doi.org/10.5194/egusphere-2025-4058
Preprint. Discussion started: 28 August 2025

Abstract

Understanding the physicochemical processes that supply atmospheric aerosol iron (Fe) to the ocean is crucial in our understanding of global biogeochemical cycles. Anthropogenic emissions contribute significant fluxes of aerosol Fe to the atmosphere, the soluble fraction of which can modulate marine primary productivity upon its deposition to the ocean surface. However, aerosol Fe solubility remains poorly constrained, due in part to a lack of direct measurements spanning a multitude of anthropogenic sources. We measured solubility of aerosol Fe from several distinct anthropogenic combustion processes and fuel types. The median Fe solubility varied widely by source, ranging from 0.03% for power plant coal fly ash to 55.87% for biofuel burning; furthermore, residential coal burning aerosol possessed much higher Fe solubility than industrial coal fly ash. Using new Fe solubilities reported herein, we updated parameters for anthropogenic aerosol Fe within the Mechanism of Intermediate complexity for Modeling Iron, an aerosol Fe module of the Community Earth System Model v2. Such updates led to significant improvement in model performance over ocean regions heavily influenced by anthropogenic emissions, and we identified residential burning as a significant source of soluble aerosol Fe to the ocean. Our work underscores the need to further refine understanding of physicochemical properties of aerosol Fe from a wide variety of anthropogenic sources. In turn, this understanding will aid in characterizing the influences of anthropogenic activities on past, present, and future atmospheric nutrient inputs to marine ecosystems.

https://doi.org/10.5194/egusphere-2025-4058
Preprint. Discussion started: 28 August 2025

1 Introduction

Anthropogenic activities have altered the atmospheric burden and deposition fluxes of biogeochemically relevant trace metals, including iron (Fe) (Bergas-Massó et al., 2023; Hamilton et al., 2020a). Fe availability in ocean waters plays a particularly important role in modulating the spatiotemporal distribution of primary productivity in ocean ecosystems, which has downstream impacts on marine fisheries and carbon sequestration (Ito et al., 2021; Tagliabue et al., 2014; Tagliabue et al., 2017). Energy-production, transportation, shipping, and manufacturing (e.g., steel production) are all characterized sources of anthropogenic aerosol Fe (Ito and Miyakawa, 2023; Ito and Shi, 2016; Rathod et al., 2024). These differing combustion fuel types possess distinct physicochemical properties that influence their impact on radiative forcing and nutrient supply (Al-Abadleh et al., 2023; Ito et al., 2018; Matsui et al., 2018; Rathod et al., 2020).

To assess the potential nutritional impact of atmospheric Fe deposition on ocean ecosystems, atmospheric aerosol research primarily focuses on tracing the soluble Fe content in aerosol (Baker et al., 2020; Ito et al., 2019; Mahowald et al., 2018). Soluble Fe content is often expressed as the fraction of soluble to total Fe in aerosol and then reported as a percentage solubility (Baldo et al., 2022; Liu et al., 2022; Mahowald et al., 2009). Several key processes control solubility of aerosol Fe over the course of its lifetime: 1) Fe mineralogy, 2) interactions with acidic and organic species in aerosol and cloud water, and 3) particle size and surface area to volume ratios (Bergas-Massó et al., 2023; Journet et al., 2008; McDaniel et al., 2019). Anthropogenic combustion not only alters the magnitude and spatial distribution of Fe fluxes to and from the atmosphere and surface ocean, but also influences the composition of the

https://doi.org/10.5194/egusphere-2025-4058
Preprint. Discussion started: 28 August 2025

atmosphere, that in turn, influences dissolution chemistry of aerosol Fe both directly and indirectly. Mixing of aerosol Fe with acidic (e.g., sulfates or nitrates) and organic species (e.g., oxalate) co-emitted during anthropogenic combustion increases its solubility during transport (Bergas-Massó et al., 2023; Chen et al., 2024; Itahashi et al., 2022; Li et al., 2017; Longo et al., 2016). Furthermore, diverse technologies utilized during combustion processes (i.e., variable combustion temperatures, boilers vs. furnaces, degree of emission control, and the fuel quality) also influence the physicochemical properties of aerosol Fe beyond the composition of fuel alone. As a result, study of how socioeconomic, technology, and policy driven changes to anthropogenic fuel-burning, is needed to anticipate impacts on the global Fe cycle (Hamilton et al., 2020a).

When compared to mineral dust, anthropogenic emissions of aerosol Fe are several orders of magnitude lower at the global scale; however, anthropogenic Fe has a higher fractional solubility (Ito et al., 2021) and source regions of dust and anthropogenic Fe are usually spatially distinct (Hamilton et al., 2020a; Hamilton et al., 2019). Therefore, anthropogenic activity can be a major contributor to Fe fluxes in many high nutrient low chlorophyll (HNLC) ocean regions (Hawco et al., 2025; Liu et al., 2022).

Despite the importance of understanding anthropogenic Fe fluxes, the fractional solubility of aerosol Fe, emitted from various anthropogenic sources, remains poorly understood (Desboeufs et al., 2005; Li et al., 2022b; Oakes et al., 2012); consequently, Fe solubility parameterizations in modeling studies for anthropogenic Fe vary widely (Ito et al., 2019; Myriokefalitakis et al., 2018). Accordingly, in this work, we measured the Fe content and solubility of aerosol emitted by several important anthropogenic sources (i.e. coal power plants,

https://doi.org/10.5194/egusphere-2025-4058
Preprint. Discussion started: 28 August 2025

steelwork industry, municipal water combustion, oil combustion, residential coal, and biofuel burning). Then, using an Earth System Model, we applied novel observational findings by updating Fe solubility parameters in distinct anthropogenic combustion fuel-sources. Modeled Fe solubilities were validated against a global observational dataset at the regional scale. We further used this model to quantify and bound uncertainties in emission and deposition fluxes of soluble Fe under three anthropogenic combustion emission scenarios spanning past (pre-industrial) to future (shared socioeconomic pathway 3-7.0) conditions.

2 Methodology

Experimental and modelling methods employed in our work are described in Sections 2.1 and 2.2, respectively.

2.1 Experimental methods

This work examined six types of anthropogenic combustion aerosol, which were classified into two broad categories. The first category, fly ash, included power plant coal fly ash, steelwork fly ash, municipal waste fly ash, and oil fly ash. The second category, residential fuel sources, included residential coal and biofuel combustion. Biofuels examined in this work were limited to straw, wood, grasses and leaves, and we did not examined other biofuels such as dung. We also studied one oil bottom ash sample, in order examine whether Fe solubility is significantly different between oil fly ash and bottom ash.

2.1.1 Fly ash and bottom ash samples

Power plant coal fly ash samples were obtained from electrostatic precipitators or baghouse rows in coal power plants in 29 provinces in China (Li et al., 2021; Liu et al., 2021); one coal power plant was selected in each province except for Guangdong and Shandong where

https://doi.org/10.5194/egusphere-2025-4058
Preprint. Discussion started: 28 August 2025

two coal power plants were selected for each province. As a result, 31 power plant coal fly ash samples were examined in total. In addition, we examined 29 steelwork fly ash samples collected from different iron and steel plants, three municipal waste fly ash samples, two oil fly ash samples (Wu et al., 2018) and one oil bottom ash sample (Fu et al., 2012). Fly ash and bottom ash samples were directly provided by these factories.

Fly ash and bottom ash samples (~10 mg for each sample) were digested and then analyzed using inductively coupled plasma mass spectrometry (ICP-MS) to determine their Fe content. Experimental procedures for sample digestion and total Fe measurement can be found elsewhere (Li et al., 2022c). Soluble Fe was leached and determined using the procedure described in our previous work (Li et al., 2022b). In brief, fly ash and bottom ash samples (~20 mg for each sample) were individually leached in 20 mL sodium acetate buffer (5 mmol/L, pH = 4.3) for 2 h, during which an orbital shaker (300 rpm) was used to stir the solution. The aqueous mixture was centrifuged (3000 rpm) for 15 min, and a pH paper (range: 3.5-6.8; precision: 0.3; Macherey-Nagel, Germany) was used to measure the pH of the solution and no measurable pH change occurred after leaching. The aqueous solution was filtered through a polyethersulfone filter (pore size: 0.22 μm), acidified to contain 1% (v/v) nitric acid and then analyzed by ICP-MS to measure soluble Fe. In this work, fractional solubility of Fe was reported as the ratio (in %) of soluble Fe to total Fe.

2.1.2 Residential coal and biofuel combustion aerosols

Generation and collection of residential coal and biofuel combustion aerosols are detailed in the supplement (Text S1). In brief, we burned coal and biofuel in a commercial cook stove which is widely used in rural areas in China, and collected $PM_{2.5}$ samples (aerosol particles

https://doi.org/10.5194/egusphere-2025-4058
Preprint. Discussion started: 28 August 2025

with aerodynamic particle diameters below 2.5 μm) onto pre-cleaned Whatman 41 (W41) cellulose filters using a medium volume aerosol sampler (TH-150C, Tianhong Co.).

Our work examined three types of coal (anthracite, semibituminous coal, and bituminous coal) and nine types of biofuel (wheat straw, rice straw, corn straw, rape straw, cogongrass, China fir trunk, pine trunk, poplar trunk, and pine needle) commonly found in China. We collected eight filter samples for each fuel type, except anthracite for which we only collected two filter samples. We had to combine some filter samples in our experimental analysis to meet the detection limit for soluble Fe; as a result, the number of effective filter samples (for which Fe content and solubility were reported) were usually <8 for each fuel type.

After aerosol collection, the filters were individually placed in a pre-cleaned Petri dish and then stored in a desiccator for 60 h to remove particle-associated water. The mass of filters before and after aerosol collection were measured (accuracy of 0.1 mg), and the mass of particles collected ranged from 2.5 to 432.7 mg. Each filter was then divided into two equal parts. To determine the soluble Fe content, the first half of a filter was leached in 20 mL sodium acetate buffer (5 mmol/L, pH = 4.3) for 2 h (Section 2.1.1) and analyzed using ICP-MS. Fe concentrations in some leaching solutions were low; as a result, these leaching solutions (~15 mL for each solution) were combined for the same fuel type and then pre-concentrated to a volume of 6 mL, in order to increase Fe concentration in the solution used for ICP-MS analysis. The second half of a filter was digested and analyzed by ICP-MS to determine total Fe, and the experimental procedure used can be found in our previous work (Zhang et al., 2022). If leaching solutions were combined for the first parts of these filters, their second parts were also combined and digested together to allow direct comparison.

https://doi.org/10.5194/egusphere-2025-4058
Preprint. Discussion started: 28 August 2025

2.2 Model simulations

2.2.1. Atmospheric Fe model description

Earth System Models can investigate the spatiotemporal distribution and fluxes of key atmospheric nutrients under various climatological regimes (Hamilton et al., 2020a; Hamilton et al., 2022; Wu et al., 2020). To test the impact of new soluble Fe parameters on modeled fluxes of soluble aerosol Fe to the atmosphere and marine ecosystems, we used the Mechanism of Intermediate complexity for Modeling Iron (MIMI). MIMI is an Fe aerosol-chemistry module embedded within the atmospheric component (Community Atmosphere Model version 6, CAM6) of the Community Earth System Model version 2 (CESM2) (Danabasoglu et al., 2020; Hamilton et al., 2019). Mineral dust, anthropogenic combustion, and wildfire emissions are currently represented as sources of aerosol Fe in MIMI. The current dust emission scheme within MIMI includes an updated soil moisture submodule within the land component of the model that prognostically calculates dust aerosolization as a function of soil moisture (Li et al., 2022a). The inclusion of these improvements to dust and updated anthropogenic Fe sources represents a new working version of MIMI v1.1, as described herein.

A comprehensive overview of MIMI model details and parameters is provided in Hamilton et al. (2019), and in brief, MIMI simulates the emission, atmospheric transport, and deposition of Fe-containing aerosol within three distinct particle size modes (Aitken, accumulation, and coarse modes). Within each source of aerosol Fe (dust, wildfire, and anthropogenic combustion), both the insoluble and soluble fractions are carried as separate tracers, and the soluble fraction of Fe for each aerosol source is assigned at the point of emission. Prior to deposition and during atmospheric transport, Fe solubility is further modified via non-

https://doi.org/10.5194/egusphere-2025-4058
Preprint. Discussion started: 28 August 2025

reversible multiphase reactions with acidic and organic species. Acidic processing is a function of aerosol pH and temperature, while organic processing is an aqueous phase chemistry reaction that depends on oxalate concentrations which are calculated based on the concentrations of secondary organic aerosol present (Johnson and Meskhidze, 2013; Scanza et al., 2018).

The model is gridded in a 3-dimensional space at a resolution of 0.96×1.25 degrees (latitude × longitude) and includes 56 vertical pressure levels from the surface to 2 hPa at the highest altitude. Meteorology is forced in all the simulations using Modern-Era Retrospective analysis for Research and Applications Version 2 (MERRA-2), and a 1-year model spin up was undertaken for all simulations.

2.2.2 Global pyrogenic Fe emission inventories and input dataset development

While dust Fe emissions are calculated prognostically within MIMI, anthropogenic and wildfire (pyrogenic) emissions were prescribed using emissions inventories. To supply initial anthropogenic Fe emission fluxes to the model, we used an annual mean emission inventory for anthropogenic combustion Fe that was first developed in Rathod et al. (2020) and further detailed in Rathod et al. (2024). In this inventory, Fe content in combustion aerosol was empirically derived for the present day (PD; climatological year 2010) using the Speciated Pollution Emissions Wizard (SPEW) (Bond et al., 2007; Bond et al., 2004) which characterized anthropogenic emissions of particulate matter by fuel-source and combustion technology. Soluble and insoluble Fe content in emissions were dependent on fuel-type and were accordingly segregated by key sectors and fuels: 1) industrial fossil fuel (coal), 2) industrial and vehicular fossil fuels (oil), 3) smelting operations (steel/iron), and 4) residential

https://doi.org/10.5194/egusphere-2025-4058
Preprint. Discussion started: 28 August 2025

cooking/heating (biofuel/biomass/wood) (Rathod et al., 2020). Industrial oil emissions were separated by land- and sea-based emissions to distinguish terrestrial transportation from shipping. Wildfire-Fe emission parameters are detailed in Hamilton et al. (2019), and in this work we use the CMIP6 (Coupled Model Intercomparison Project phase six) fire emission datasets for PD simulations (van Marle et al., 2017).

For the first time, we segregated anthropogenic coal Fe sources into industrial and residential coal burning sources. In the dataset provided by Rathod et al. (2020), Fe from the coal source was assumed to only stem from industrial activity, but here we isolate the residential source. This segregation was achieved by applying a spatially resolved (on the Earth System Model grid box co-ordinates) ratio of industrial-to-residential coal that was calculated based on the ratio of industrial-to-residential black carbon (BC) emissions within the CMIP6 dataset (Hoesly et al., 2018), and this calculation assumed that the Fe-to-BC ratios were matched between sources.

2.2.3 Model simulations performed

Ten model simulations were performed to evaluate the impact of changes to Fe solubility of anthropogenic combustion aerosol (Section 2.1) on atmospheric soluble Fe fluxes to key marine ecosystems (Table 1). For all simulations, we set the model climatology to present-day (PD) conditions spanning 2009-2011. Simulations were distinguished as cases (with variable Fe solubility parameterizations) within different emission scenarios (with variable anthropogenic combustion emission fluxes).

https://doi.org/10.5194/egusphere-2025-4058
Preprint. Discussion started: 28 August 2025

Table 1. Description of model simulations performed using MIMI with emission scenarios and emissions inventory (database). PD = present day (2010 CE), PI = pre-industrial (1750 CE), SSP370 = shared socioeconomic pathway scenario 3-7.0, MID = midcentury (2040-2050 CE) and END = end century (2090-2100 CE). NA = assumed industrial activity is zero at 1750 CE.

Emissions Scenario	Simulation	BC Emissions database	BC Emission (Tg a^{-1})
PD	PD-BASE	CMIP6	6.46
PD	PD-RESI	CMIP6	6.46
PD	PD-BIOF	CMIP6	6.46
PD	PD-IND	CMIP6	6.46
PI	PI-BASE	NA	NA
PI	PI-RESI	NA	NA
FU (2050)	MID-SSP370-BASE	SSP3.70	8.30
FU (2050)	MID-SSP370-BIOF	SSP3.70	8.30
FU (2100)	END-SSP370-BASE	SSP3.70	6.33
FU (2100)	END-SSP370-BIOF	SSP3.70	6.33

Four PD simulations aimed to assess the impact of each new solubility parameter on the ability of the model to capture ship-based observations of total Fe, soluble Fe and Fe solubility. These simulations utilized the anthropogenic combustion emission inventory representing PD emissions as described in Section 2.2.2. The first PD case (PD-BASE) served as a baseline, i.e. no changes were made to anthropogenic Fe solubilities when compared to previous studies using MIMI to model global Fe fluxes (Rathod et al., 2020; Rathod et al., 2024). In the next three PD cases (PD-RESI, PD-BIOF, PD-IND), fractional solubility was updated incrementally for individual sectors to assess fuel-type specific impacts to soluble Fe fluxes, which are later detailed in Section 3.3. Information on model validation and constraint to ship-based observations of aerosol Fe is provided in Section 2.2.5.

https://doi.org/10.5194/egusphere-2025-4058
Preprint. Discussion started: 28 August 2025

Using both pre-industrial (PI; 1750 CE) and future (FU; 2050 and 2100 CE) anthropogenic emissions scenarios, we performed six additional model simulations using the -BASE and -BIOF solubility parameters applied during the PD simulations; these solubility cases were selected based on model validation results as presented in Section 3.3. To isolate how changes in soluble aerosol Fe fluxes responded to changes in emission parameterizations and subsequent dissolution chemistry, PI and FU simulations were conducted with meteorological and climatological conditions identical to PD (2009-2011). Emissions inventories (including Fe) were modified to represent PI and future FU projections for atmospheric emissions.

PI-BASE and PI-BIOF served as a baseline for comparison to PD and FU simulations, with minimal influence on the Fe cycle by anthropogenic emissions (Table 1). In the PI era, Fe emissions were predominantly natural in source (e.g., dust and wildfire), and only residential biofuel burning was represented as an anthropogenic source of Fe (Hamilton et al., 2020b). All other anthropogenic sources of Fe were assumed to be zero.

MID-SSP370-BASE, MID-SSP370-BIOF, END-SSP370-BASE, and END-SSP370-BIOF were conducted to evaluate the projected impact of socioeconomic changes to energy production and fuel-usage in communities across the globe, as well as population increases. We chose to utilize the emissions scenario detailed in the Shared Socio-economic Pathway 3-7.0 “regional rivalry ” (SSP370), which represents anticipated sociopolitical and environmental changes resulting in an increase to radiative forcing by 3-7.0 W m^{-2} by the year of 2100 (Riahi et al., 2017). In this scenario, air pollutants sourced from anthropogenic activity are projected to be highest when compared to alternative SSP scenarios (SSP126, SSP245, and SSP585). Accordingly, model simulations using SSP370 can be leveraged to establish an upper

https://doi.org/10.5194/egusphere-2025-4058
Preprint. Discussion started: 28 August 2025

bound estimate for future soluble aerosol Fe fluxes from anthropogenic combustion emissions. Dust fluxes in future Fe emission scenarios were adjusted to account for dust-climate feedback using a scaling factor ranging between 1.0-1.1, as described in Hamilton et al. (2020b). Given that BC emissions are anticipated to peak in the midcentury (2040-2050) but return to PD-comparable emissions by 2100 (Turnock et al., 2020), we assessed projected changes to Fe emissions at both the mid-point (2050) and endpoint of the 21st century (2100).

2.2.4 Preindustrial (PI) and future (FU) Fe emission estimates

For PI simulations, we used a pre-developed Fe combustion emission inventory (Hamilton et al., 2020a). Only residential biofuel burning served as an anthropogenic source of Fe due to a presumable lack of industrialized anthropogenic emissions (i.e., fossil fuels and smelting); global emission was 0.7×10^{-3} Gg Fe a^{-1} and only occupied the fine aerosol mode (i.e., sum of Aitken and accumulation modes). Details on the development of the PI Fe combustion emission inventory are provided in Hamilton et al. (2020a). The SimFire inventory, coupled to the LPJ-GUESS (Lund-Potsdam-Jena General Ecosystem Simulator) vegetation model, was used to prescribe wildfire-Fe emissions during the PI era (Hamilton et al., 2018; Hamilton et al., 2020a; Knorr et al., 2016).

For FU simulations, we developed two new Fe emissions datasets which were derived from our PD dataset and linearly scaled for all combustion sources according to projected changes in anthropogenic BC emissions via CMIP6 anthropogenic BC emission dataset (Hoesly et al., 2018; Riahi et al., 2017). In the CMIP6 BC inventory, emissions are segregated by the following sectors: agriculture, energy, industrial, terrestrial transportation, residential/commercial/other, solvents production and application, waste, and international

https://doi.org/10.5194/egusphere-2025-4058
Preprint. Discussion started: 28 August 2025

shipping. We treated 'energy' and 'industrial' sources together as industrial coal BC sources and ocean-masked 'international shipping' with land-masked 'terrestrial transportation' together as oil BC sources. BC emissions labeled 'residential, commercial and other' were separated into residential coal and residential biofuel sources of BC based on the grid-cell specific ratios of residential coal Fe to residential biofuel Fe in our PD Fe emissions dataset. BC emissions from smelting operations were not directly available for PI or FU projections; therefore, they were set to 0 in the PI and maintained at PD levels in the FU.

Once FU BC emissions were organized according to combustion fuel-sources as characterized herein, using a dynamic ratio of Fe-to-BC dependent on region, fuel-source emission sector, and aerosol size fraction, we calculated scenario-specific Fe emissions in individual grid cells using Eq. (1):

$$\frac{[Fe_X]_{i,j,a,b}}{[BC_X]_{i,j,a,b}} = \frac{[Fe_{PD}]_{i,j,a,b}}{[BC_{PD}]_{i,j,a,b}} \qquad (1)$$

where X denotes the emissions scenario (MID-SSP370 or END-SSP370), i and j represent the longitudinal and latitudinal coordinates, a represents the aerosol mode (fine or coarse), b represents the fuel-source (industrial oil, industrial coal, residential coal, residential biofuel, or smelting), and [Fe] and [BC] represent the fluxes (kg m^{-2} s^{-1}) of Fe and BC, respectively. Using these gridded emissions, fuel-sources were then summed and segregated by soluble fraction to generate six combustion-Fe tracers to be read into and transported within the model, distinguished by aerosol size and solubility as calculated using Eqs. (2-3):

$$[Fe_{insol}]_a = \Sigma \{[Fe_X]_{i,j,a,b} * (1 - sol_b)\} \qquad (2)$$

$$[Fe_{sol}]_a = \Sigma \left([Fe_X]_{i,j,a,b} * sol_b\right) \qquad (3)$$

https://doi.org/10.5194/egusphere-2025-4058
Preprint. Discussion started: 28 August 2025

where *insol* represents the insoluble fraction, *sol* represents the soluble fraction, and sol_b represents the fractional solubility for each fuel-source (*b*). As a final step, the fine mode was split into accumulation and Aitken modes by applying a simple ratio of 9:1.

For wildfire-Fe emissions in FU scenarios, we used the CMIP6 fire emission datasets for each respective simulation, i.e. MID-SSP370 and END-SSP370 (Bergas-Masso et al., 2025; Hamilton et al., 2024).

2.2.5 Model validation

To evaluate model performance, we compared global observations of total Fe concentration, soluble Fe concentration, and Fe solubility to modeled values for each PD simulation, grouping data by key aerosol deposition and ocean biogeochemistry regions. The observational dataset of Fe content in aerosol was reported in Hamilton et al. (2019) and updated herein to include measurements published between 2021 and 2024 (n = 1624). Observed Fe solubility in aerosol spans five orders of magnitude (Perron et al., 2024), and one reason for this large range is due to differences in experimental procedures during quantification (Tang et al., 2025). To facilitate a more direct comparison between modelled and observed soluble Fe content, we removed observations from the global dataset that did not measure soluble Fe directly. When multiple observations fell within a model grid cell, values were aggregated to climatological averages, using medians to be most representative of expected variations in Fe fluxes across time and space (final n = 990; Figure S3). For final evaluation of the model capability in simulating surface Fe concentrations, both model and observational data were grouped into key ocean regions (Figure 1), based on predominant

https://doi.org/10.5194/egusphere-2025-4058
Preprint. Discussion started: 28 August 2025

sources of atmospheric aerosol and phytoplankton nutrient limitation dynamics (i.e., HNLC regions) as revealed in Hamilton et al. (2019) and Hamilton et al. (2023).

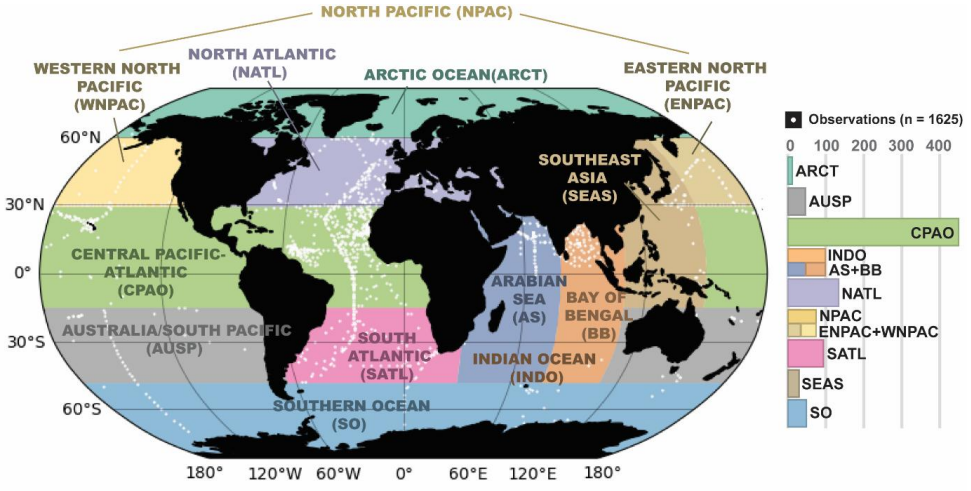

Figure 1. Regional groupings for model-observation comparisons of surface Fe concentrations (ship-based, in aerosol). The coordinates for individual Fe observations are indicated with a white circle. Number of soluble Fe observations within each region are provided by the histogram.

3 Results and Discussion

Sections 3.1 and 3.2 present Fe content and solubility measured in our experimental work, and modeling results are presented in Section 3.3.

3.1 Fe content by fuel type

This work quantified the Fe content in particles from six different combustion and anthropogenic sources, including power plant coal fly ash, residential coal combustion aerosol, steelwork fly ash, residential biofuel burning aerosol, municipal waste fly ash, and oil fly ash (Table 2; Fe content in individual samples is provided in Tables S1-S5).

https://doi.org/10.5194/egusphere-2025-4058
Preprint. Discussion started: 28 August 2025

346

347 **Table 2.** Summary of Fe content and solubility for power plant coal fly ash, residential coal
348 combustion aerosol, steelwork fly ash, biofuel burning aerosol, municipal waste fly ash, oil fly
349 ash and oil bottom ash examined in our work (*n*: number of samples examined in our work).

sample type	*n*	range	average	median
Fe content (mg/g)				
power plant coal fly ash	31	20.7-103.8	37.2±16.8	35.0
residential coal combustion aerosol	10	0.025-0.101	0.044±0.023	0.038
steelwork fly ash	29	5.8-918.9	312.6±246.1	346.5
biofuel burning aerosol	27	0.002-0.101	0.023±0.026	0.013
municipal waste fly ash	3	3.9-29.7	18.7±13.3	22.6
oil fly ash	2	9.1-18.3	13.7±4.6	13.7
oil bottom ash	1	-	191	191
Fe solubility (%)				
power plant coal fly ash	31	0.002-0.17	0.05±0.05	0.03
residential coal combustion aerosol	10	7.03-100	33.30±27.71	28.45
steelwork fly ash	29	0.007-10.64	1.37±2.77	0.07
biofuel burning aerosol	28	2.86-100	56.07±30.95	55.87
municipal waste fly ash	3	0.58-2.41	1.51±0.92	1.54
oil fly ash	2	11.70-13.43	12.56±0.87	12.56
oil bottom ash	1	-	25.47	25.47

350

351

https://doi.org/10.5194/egusphere-2025-4058
Preprint. Discussion started: 28 August 2025

3.1.1 Power plant coal fly ash

Fe content ranged from 20.7 to 103.8 mg/g for the 31 power plant coal fly ash samples examined in our work, with average and median values being 37.2 ± 16.8 and 35.0 mg/g, respectively. As shown in Table S6, Fe content ranged from 16.0 to 52.0 mg/g (n = 3) in one study (Baldo et al., 2022), with mean and median values being 33.0 ± 18.0 and 31.0 mg/g; in another study (Goodarzi, 2006), the median value of Fe content was determined to be 34.4 mg/g (n = 7). Fe content measured by these two studies (Baldo et al., 2022; Goodarzi, 2006) agreed well with our work. Some other studies (Dutta et al., 2009; Fu et al., 2012; Jankowski et al., 2006; Meij, 1994) found higher mean or median Fe content for power plant coal fly ash (Table S6), but the reported ranges overlapped with our work. For example, Fe content were found to range from 38.3 to 98.6 mg/g (n = 7) in one study (Li et al., 2022b), with mean and median values being 62.1 ± 26.7 and 43.2 mg/g; in another study (Moreno et al., 2005), Fe content were found to range from 18.2 to 112.0 mg/g (n = 23), with mean and median values being 57.8 ± 22.7 and 52.5 mg/g.

In summary, the mean or median Fe content reported in different studies are typically in the range of 30-70 mg/g for power plant coal fly ash, and this variability is likely due to difference in coal (Wang et al., 2015; Ward, 2016) and combustion conditions (Blissett and Rowson, 2012; Kutchko and Kim, 2006). Fe content in power plant coal fly ash was set to ~70 mg/g in some modeling studies (Luo et al., 2008; Rathod et al., 2020), being consistent with experimental results.

https://doi.org/10.5194/egusphere-2025-4058
Preprint. Discussion started: 28 August 2025

3.1.2 Residential coal combustion aerosol

For the 10 residential coal combustion aerosol samples ($PM_{2.5}$) we examined, Fe content ranged from 0.025 to 0.101 mg/g (Table 2), with average and median values being 0.044 ± 0.023 and 0.038 mg/g, respectively. Only a few previous studies measured Fe content in residential coal combustion aerosols (Table S6). The average Fe content was determined by Patil et al. (2013) to be 0.048 ± 0.035 mg/g (n = 3) for $PM_{2.5}$ and 0.061 ± 0.044 mg/g (n = 3) for PM_{10}, being similar to or slightly higher than our result. In another two studies (Watson et al., 2001; Zhang et al., 2012), the average Fe content was measured to be 0.671 ± 0.023 mg/g (n = 4) and 0.7 ± 0.1 mg/g (n = 5), significantly higher than our result, and such differences may be attributed to variations in coal types and combustion conditions. Overall, our and previous studies suggest that the Fe content in residential coal combustion aerosols is very low, typically below 1 mg/g. Fe content were set to 1 and 0.5 mg in previous modeling studies (Luo et al., 2008; Rathod et al., 2020), being broadly consistent with experimental results.

Fe content in power plant coal fly ash is much higher than residential coal combustion aerosols, primarily due to differences in combustion conditions (Rathod et al., 2020). Power plant coal fly ash has very low carbon content and is mainly composed of metals and minerals (Ahmaruzzaman, 2010; Li et al., 2022c; Patil et al., 2013); in contrast, residential coal combustion aerosol particles contain a large fraction of carbonaceous materials due to incomplete combustion, and thus the content of metals, including Fe, are much lower (Patil et al., 2013; Zhang et al., 2012). Furthermore, combustion temperature typically ranges from 1200 to 1700 ºC for coal-fired power plant, enabling Fe in coal to enter fly ash particles through volatilization-condensation (Blissett and Rowson, 2012); residential coal combustion occurs at

https://doi.org/10.5194/egusphere-2025-4058
Preprint. Discussion started: 28 August 2025

much lower temperatures which are insufficient for Fe to enter aerosols through this process (Rathod et al., 2020), also leading to lower Fe content.

3.1.3 Steelwork fly ash

For the 29 steelwork fly ash samples we examined, Fe content ranged from 5.8 to 918.9 mg/g, with mean and median values measured to be 312.6 ± 246.1 and 346.5 mg/g, respectively (Table 2). As shown in Table S6, some previous studies have reported average Fe content to be 358.9 (n = 1), 369.3 (n = 1), 312.2 (n = 1), and 329.1 ± 22.6 mg/g (n = 4) (Alizadeh and Momeni, 2016; Silva et al., 2019; Souza et al., 2010; Vieira et al., 2013), in good agreement with our results. Lower Fe content was also reported by previous work, with average values being 86.0 (n = 1), 128.1 (n = 1), 150.8 (n = 1), 286.5 (n = 1), 284.6 (n = 1), 238.7 (n = 1), and 267.3 ± 4.8 mg/g (n = 4) (Al-Negheimish et al., 2021; Alsheyab and Khedaywi, 2016; Laforest and Duchesne, 2006; Li et al., 2023; Loaiza et al., 2017; Stathopoulos et al., 2013; Xia and Picklesi, 2000); in contrast, some previous studies also found the average or mean Fe content to be around 400-500 mg/g (Machado et al., 2006; Patil et al., 2013; Ye et al., 2021), slightly higher than our results.

Despite some variability in Fe content reported by our and previous studies (Table S6), the mean or median Fe content are generally around 300–500 mg/g for steelwork fly ash. In a recent modeling study (Rathod et al., 2020), the Fe content in steelwork fly ash was set to 440 mg/g (and the lower and upper bounds were set to 150 and 950 mg/g), being consistent with experimental results.

https://doi.org/10.5194/egusphere-2025-4058
Preprint. Discussion started: 28 August 2025

3.1.4 Biofuel burning aerosol

Our work considered biofuel burning aerosols for nine types of biofuels, including four types of crop straw, one type of wild grass, and four types of wood. Fe content in biofuel burning aerosols ranged from 0.002 to 0.101 mg/g (Table 2), with average and median values being 0.023 ± 0.026 and 0.013 mg/g, respectively. As shown in Table S6, the average Fe content was determined to be 0.024 ± 0.017 mg/g (n = 3) for $PM_{2.5}$ (Patil et al., 2013), very close to our result; in another study (Hildemann et al., 1991), it was determined to be 0.090 mg/g for PM_2 (n = 2), higher than our result. In some other studies, average Fe content were reported to be in the range of 0.162-0.440 mg/g for $PM_{2.5}$ (Alves et al., 2011; Hedberg et al., 2002; Watson et al., 2001; Zhang et al., 2012) and 0.723 ± 0.661 mg/g for PM_{10} (Schmidl et al., 2008), much higher than our results.

Fe content in biofuel burning aerosols showed large variability in different studies, likely due to variations in combustion conditions and biofuel types. For example, metal content in biofuel burning aerosols depended greatly on biofuel types and regions where biofuel was collected (Goncalves et al., 2010), and aerosol particles emitted by wild grass combustion contained larger amounts of metal than wood combustion (Jahn et al., 2021). Modeling studies have used a similar distribution of Fe content between 0.2 and 0.580 mg/g for biofuel burning aerosols (Luo et al., 2008; Rathod et al., 2020).

3.1.5 Municipal waste fly ash, oil fly ash and oil bottom ash

For the three municipal waste fly ash samples we investigated, Fe content ranged from 3.9 to 29.7 mg/g, with average and median values being 18.7 ± 13.3 and 22.6 mg/g (Table 2). Several previous studies measured Fe content in municipal waste fly ash (Table S6). For

https://doi.org/10.5194/egusphere-2025-4058
Preprint. Discussion started: 28 August 2025

example, the average Fe content were measured to be 18.0 ± 13.3 mg/g (n = 3) and 23.1 mg/g (n = 1) in two studies (Cobo et al., 2009; Raclavská et al., 2017), very similar to our results; another four studies (Funari et al., 2017; Liu et al., 2009; Wu and Ting, 2006; Wu et al., 2012) reported lower Fe content, ranging from 5.2 to 10.9 mg/g; some other studies (Bayuseno and Schmahl, 2011; Lin et al., 2003; Wan et al., 2006; Zhang et al., 2011) also reported slightly higher Fe content, ranging from 27.1 to 34.3 mg/g. In summary, most studies suggest that Fe content in municipal waste fly ash are around 20 mg/g, and it has been set to 18.8 mg/g in a modeling study (Rathod et al., 2020), being consistent with experimental results.

Fe content in the two oil fly ash samples we examined were measured to be 9.1 and 18.3 mg/g, and the average value was determined to be 13.7 ± 4.6 mg/g. The Fe content was measured to be 15.0 mg/g for one oil fly ash sample (Celo et al., 2015), close to the value we reported. In another two studies (Agrawal et al., 2008; Sippula et al., 2014), the average Fe content was measured to be 1.98 ± 0.35 (n = 4) and 1.60 ± 1.21 mg/g (n = 14), lower than our result. In a modeling study (Rathod et al., 2020), the Fe content was set to 10 mg/g for oil fly ash, being consistent with the experimental results reported by our work and Celo et al. In addition, in our work the Fe content was measured to be 191 mg/g for one heavy oil bottom ash sample, much higher than that for oil fly ash.

3.1.6 Fe contents: comparison of anthropogenic and dust Fe

Figure 2a displays Fe content for anthropogenic particles examined in our current study, and the brown dashed line represents the average Fe content of desert dust (35 mg/g) (Taylor and McLennan, 1995). Steelwork fly ash has very high Fe content (median: 346.5 mg/g), about one order of magnitude higher than desert dust. Power plant coal fly ash (median: 35.0 mg/g)

https://doi.org/10.5194/egusphere-2025-4058
Preprint. Discussion started: 28 August 2025

has similar Fe content to desert dust, while municipal waste fly ash (median: 22.6 mg/g) and oil fly ash (median: 13.7 mg/g) have relatively lower Fe content than desert dust. Compared to desert dust, Fe content were around three orders of magnitude lower for residential coal and biofuel burning aerosol (median: 0.038 and 0.013 mg/g, respectively). The Fe content was much lower for residential coal and biofuel burning aerosol, likely due to lower combustion temperatures. When combustion occurs at lower temperature, the carbon content of emitted particles is higher; in addition, lower combustion temperature is not sufficient to enable Fe in the fuel to enter emitted particles via volatilization-condensation processes.

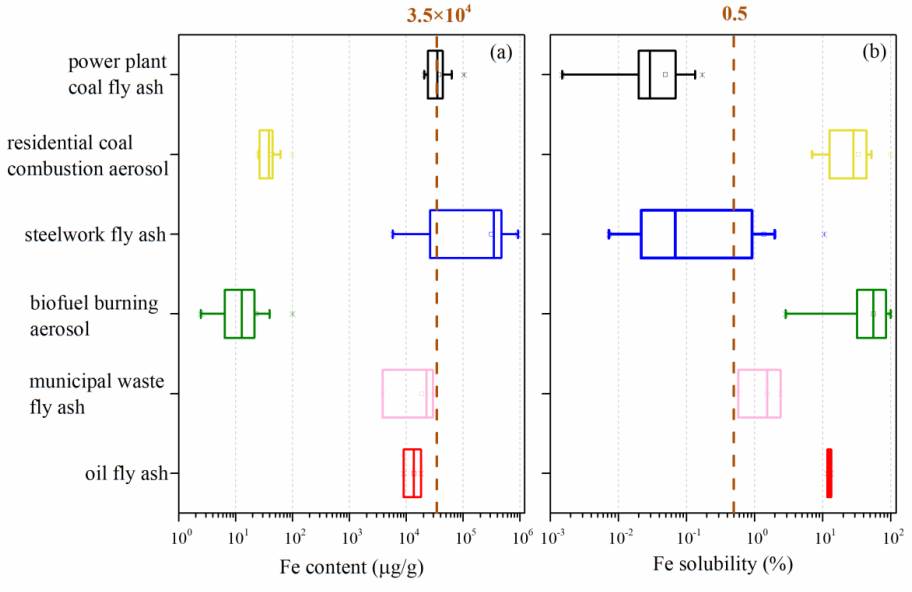

Figure 2. Fe content (a) and solubility (b) measured in our work for power plant coal fly ash, residential coal combustion aerosol, steelwork fly ash, biofuel burning aerosol, municipal waste fly ash and oil fly ash. The two brown dash lines represent (a) the Fe content (3.5×10^4 μg/g) and (b) Fe solubility (~0.5%) for desert dust, respectively.

https://doi.org/10.5194/egusphere-2025-4058
Preprint. Discussion started: 28 August 2025

3.2 Fe solubility by fuel type

3.2.1 Power plant coal fly ash

Fe solubility in acetate buffer (pH: 4.3) was found to range from 0.002% to 0.17% for power plant coal fly ash (Table 2), with the average and median values being 0.05 ± 0.05% and 0.03%, respectively. A few previous studies measured Fe solubility of power plant coal fly ash in weakly acidic or circumneutral solutions (Table S7). For example, Fe solubility was measured to be 0.06% in deionized water (Oakes et al., 2012), similar to our result; it was measured to be 0.2% in dilute sulfuric acid solution (pH: 4.7) (Desboeufs et al., 2005), slightly higher than our result; the median Fe solubility was determined to be 0.13% in acetate buffer (pH: 4.3) and 0.06% in deionized water (Li et al., 2022b), both higher than the median value we obtained. Overall, our work and previous studies suggest that Fe solubility is low in weakly acidic and circumneutral solutions for power plant coal fly ash, with mean or median values around 0.1%.

Some studies also measured Fe solubility of power plant coal fly ash in highly acidic solutions and found them to be much higher than those in weakly acidic and circumneutral solutions. For example, Fe solubilities were found to be in the range of 20-25% at pH of 1-2 (Chen et al., 2012), 4.2-8.3% at pH of 2 (Fu et al., 2012), and >40% at pH of 2.1 (Baldo et al., 2022). Although Fe solubility measured in strongly acidic solutions may not reflect initial Fe solubility, these studies suggested that acid processing in the emission plume or wider atmosphere could greatly increase Fe solubility for power plant coal fly ash.

https://doi.org/10.5194/egusphere-2025-4058
Preprint. Discussion started: 28 August 2025

3.2.2 Residential coal combustion aerosol

Fe solubility in acetate buffer (pH: 4.3) was determined to range from 7.03% to 100% for residential coal combustion aerosol (Table 2), with the average and median values being 33.30 ± 27.71% and 28.45%, respectively. To our knowledge, no previous study has measured Fe solubility for residential coal combustion aerosol. Compared to power plant coal fly ash, Fe solubility was much higher for residential coal combustion aerosol, and such difference can be attributed to much higher temperature in power plant coal combustion than residential coal combustion. Pyrite (FeS_2) is the major Fe-containing mineral in coal (Deng et al., 2015; Oliveira et al., 2016; Rathod et al., 2020). In low-temperature combustion, pyrite is mainly transformed to Fe sulfate (Bhargava et al., 2009) which has very high Fe solubility; as the temperature increases to >1000 K, Fe sulfate is further transformed to hematite and magnetite which exhibit very low solubility (Hu et al., 2006; Ram et al., 1995; Rathod et al., 2020). A previous study (Rathod et al., 2020) used the relationship between combustion temperature and Fe mineralogy in emitted particles to estimate Fe solubility for different combustion aerosols, and Fe solubility was estimated to be as high as ~32.5% for residential coal combustion aerosols, in good agreement with our experimental results.

3.2.3 Steelwork fly ash

Fe solubility in acetate buffer (pH: 4.3) was determined to range from 0.01% to 10.64% for steelwork fly ash (Table 2), and the average and median values were 1.37 ± 2.77% and 0.07%, respectively. We note that Fe solubility was significantly higher (0.92%-8.59%) for 8 samples and very low (<0.5%) for the other 21 samples (Table S3), most of which showed Fe solubility below 0.1%. No previous work has measured Fe solubility for steelwork fly ash. Our

https://doi.org/10.5194/egusphere-2025-4058
Preprint. Discussion started: 28 August 2025

experimental results were supported by a modeling study (Rathod et al., 2020) which suggested that the major Fe-containing species in steelwork fly ash were Fe oxides with very low Fe solubilities.

3.2.4 Biofuel burning aerosol

For biofuel burning aerosol, Fe solubility in acetate buffer (pH: 4.3) ranges from 2.86% to 100% with average and median values of 56.07 ± 30.95% and 55.87%, respectively (Table 2). Based on the relationship between combustion temperature and Fe-containing species in emitted aerosols, Fe solubility was previously estimated at 35% for wood burning (i.e., biofuel) aerosol (Rathod et al., 2020), in good agreement with our experimental results.

The biofuel examined in our experiment was burnt in a sealed stove and contained no apparent local soil contamination. As such, these results are most representative of domestic biofuel combustion for which the influence of soil-derived Fe can be expected to be negligible. In contrast, wildfires represent dynamic open fire systems that emit aerosol Fe in both fine and coarse fractions (Hamilton et al., 2019). During wildfire combustion, not only is the biofuel (biomass) consumed, but local soils are also entrained into the smoke plumes (Hamilton et al., 2022; Tegler et al., 2023). These soil-derived particles are typically larger (in particle size) and less soluble than their biofuel-derived counterparts (Hamilton et al., 2022), resulting in a larger mass of emitted Fe, albeit with a lower overall Fe solubility. Future studies would benefit from capturing emissions from open burning scenarios to better characterize the properties of wildfire-emitted Fe.

https://doi.org/10.5194/egusphere-2025-4058
Preprint. Discussion started: 28 August 2025

3.2.5 Municipal waste fly ash, oil fly ash and oil bottom ash

Fe solubility in acetate buffer (pH: 4.3) was determined to range from 0.58% to 2.41% for municipal waste fly ash (Table 2), with average and median values being 1.51 ± 0.92% and 1.54%, respectively. Few previous studies measured Fe solubility for municipal waste fly ash. Fe solubility was estimated to be <2% for municipal waste fly ash when combustion temperature exceeded 1100 K (Rathod et al., 2020), agreeing with our experimental results.

Fe solubility in acetate buffer (pH: 4.3) was determined to be 11.70% and 13.43% for the two oil fly ash samples we examined, with an average value of 12.56 ± 0.87%. In previous work, Fe solubility was measured to be 35.7% at pH of 4.7 (Desboeufs et al., 2005) and 70% in deionized water (Schroth et al., 2009), both higher than our results. Although Fe solubility measured in different studies showed some variations, all the studies suggested that oil fly ash exhibited very high Fe solubility. Moreover, Fe solubility in acetate buffer (pH: 4.3) was measured in our work to be 25.47% for one heavy oil bottom ash.

3.2.6 Fe solubilities: comparison of anthropogenic and dust Fe

Figure 2b compares our measured Fe solubility for six types of combustion and anthropogenic particles with that for desert dust. Biofuel burning aerosols (median: 55.87%), residential coal combustion aerosols (median: 28.45%), and oil fly ash (median: 12.56%) exhibited very high Fe solubility. Compared to desert dust, for which Fe solubility is around 0.5% (Chuang et al., 2005; Li et al., 2022b; Ooki et al., 2009; Schroth et al., 2009; Shi et al., 2011), Fe solubility was also higher for municipal waste fly ash (median: 1.54%) but lower for steelwork fly ash (median: 0.07%) and power plant coal fly ash (median: 0.03%).

https://doi.org/10.5194/egusphere-2025-4058
Preprint. Discussion started: 28 August 2025

Overall, Fe solubility in emitted particles was significantly higher for low-temperature combustion (residential and biofuel burning aerosols) than high-temperature combustion (municipal waste fly ash, steelwork fly ash, and power plant coal fly ash). This is because Fe in emitted particles is mainly highly soluble Fe sulfates for low combustion (Bhargava et al., 2009; Rathod et al., 2020) but Fe oxides with very low solubility for high temperature combustion (Hu et al., 2006; Ram et al., 1995; Rathod et al., 2020). The outlier to this is oil fly ash which was emitted by high temperature combustion but showed high Fe solubility. This is probably because heavy oil has high sulfur content, leading to the formation of sulfuric acid in combustion that can condense onto co-emitted Fe oxide particles and form highly soluble Fe sulfate (Rathod et al., 2020; Sippula et al., 2009).

3.3 Modeling Results

Leveraging combustion Fe solubilities as measured in aerosol emitted from combustion of different fuel sources (residential coal, industrial coal, oil, and residential biofuel), as reported in Sections 3.1 and 3.2, we performed a series of Earth System Model simulations that tested variable anthropogenic Fe solubilities at the point of emission. To pair observed solubilities (Table 2) with fuel-types represented in the model, we updated Fe emission solubility in industrial coal from 0.2 to 0.05%, in residential coal from 0.2 to 33%, in residential biofuel burning from 10 to 56%, and in oil from 38 to 25% (Table 3). Smelting Fe solubility at point of emission was kept at 0.03%, since new experimental data do not suggest an alternative solubility. New solubility parameters were applied to both fine and coarse modes within MIMI. A description of the fractional solubilities applied to each anthropogenic fuel type within each model simulation is provided in Table 3.

https://doi.org/10.5194/egusphere-2025-4058
Preprint. Discussion started: 28 August 2025

Table 3. Fractional Fe solubilities applied in each model simulation to reflect experimental findings. Rows highlighted in gray indicate baseline simulations with no changes made to Fe solubility from previous work using MIMI. To underscore modifications between simulations, a dash (–) is provided where assigned solubility did not differ from the PD-BASE simulation.

Simulation	Fe solubility modifications by fuel-type (%)				
	Industrial Coal	Residential Coal	Oil	Residential Biofuel	Smelting
PD-BASE	0.2	0.2	38	10	0.003
PD-RESI	-	33	-	-	-
PD-BIOF	-	33	-	56	-
PD-IND	0.05	33	25	56	-
PI-BASE	NA	NA	NA	10	NA
PI-BIOF	NA	NA	NA	56	NA
MID-SSP370-BASE	0.2	0.2	38	10	0.003
MID-SSP370-BIOF	-	33	-	56	0.003
END-SSP370-BASE	0.2	0.2	38	10	0.003
END-SSP370-BIOF	-	33	-	56	0.003

3.3.1 Impacts on global soluble Fe distribution

By updating Fe solubility for four distinct anthropogenic fuel-types in MIMI, our model simulations revealed a new range of potential soluble Fe fluxes to the modern ocean. When compared to PD-BASE, in the PD-RESI case soluble Fe fluxes to the surface ocean increased by 33 Gg a^{-1} (92% increase) globally, with the largest increase in emissions stemming from China, India, Australia, the USA, central Europe, and South Africa (Figure 3). These increases follow previous reports of relatively large anthropogenic emissions from these regions when compared to global averages (Rathod et al., 2024; Wang et al., 2015).

https://doi.org/10.5194/egusphere-2025-4058
Preprint. Discussion started: 28 August 2025

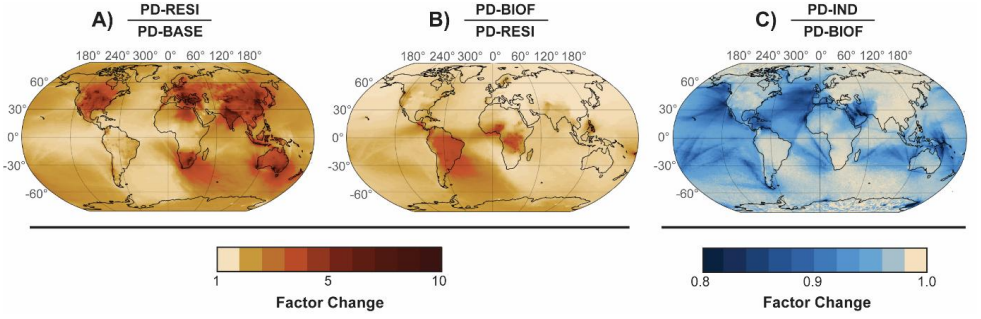

Figure 3. Relative changes to soluble Fe deposition fluxes following modifications to anthropogenic Fe solubilities in MIMI: A) residential coal, B) residential biofuel, and C) industrial (fossil fuels and oil). Note the difference in scales between A/B and C; red tones (A and B) indicate relative increases and blue tones (C) indicate relative decreases.

When we increased Fe solubility for residential biofuel in the model (PD-BIOF), soluble Fe fluxes to the ocean increased by an additional 11 Gg a^{-1}, totaling an increase of 44 Gg a^{-1} compared to PD-BASE (Table 4). Changes to soluble Fe fluxes in this case were most concentrated across the South Atlantic (Figure 3), likely due to elevated emissions (as high as a factor of 4) along the eastern coast of South America and in sub-Saharan Africa where biofuel-burning in cook stoves is a common residential practice (García-López et al., 2025; Stoner et al., 2021). When both residential coal and biofuel Fe solubilities were increased (PD-BIOF), we report a maximum change in soluble Fe fluxes, with deposition to the ocean doubling from 40 to 80 Gg a^{-1} at the global scale (123% increase relative to PD-BASE; Table 4). Both our minimum (PD-BASE) and maximum (PI-BIOF) estimates fell within previous ranges of uncertainty as reported for anthropogenic Fe deposition fluxes to the ocean (Hamilton et al., 2023; Ito and Miyakawa, 2023), suggesting that solubility modifications applied herein

https://doi.org/10.5194/egusphere-2025-4058
Preprint. Discussion started: 28 August 2025

608 aligns well with previous constraints for global soluble Fe fluxes by Earth System Models.
609 Altering Fe solubility for industrial coal (PD-IND) had a much smaller impact on soluble Fe
610 deposition fluxes to the ocean, only resulting in a 2.2 Gg a^{-1} decrease (3% decrease) at the
611 global scale. These losses in fossil-fuel based Fe emissions were distributed across multiple
612 regions but most apparent within major shipping lanes (Figure 3).

613

614 **Table 4.** Global anthropogenic combustion Fe emission and deposition fluxes (Gg a^{-1}) in the
615 preindustrial (PI), present day (PD), and Future (FU), as simulated by MIMI.

Emission Scenario	Model Simulation (case)	Fe Content	Global Emission	Global Deposition	Deposition to Ocean
PI (1750 CE)	PI-BASE	Total	0.8	0.8	0.3
		(Soluble)	(0.08)	(0.1)	(0.04)
	PI-BIOF	Total	0.8	0.8	0.3
		(Soluble)	(0.44)	(0.5)	(0.2)
PD (2010 CE)	PD-BASE	Total	2220	2220	590
		(Soluble)	(20)	(90)	(40)
	PD-BIOF	Total	2220	2220	590
		(Soluble)	(170)	(270)	(80)
FU (2050 CE)	MID-SSP370-BASE	Total	2400	2400	620
		(Soluble)	(20)	(90)	(40)
	MID-SSP370-BIOF	Total	2400	2400	620
		(Soluble)	(180)	(250)	(80)
FU (2100 CE)	END-SSP370-BASE	Total	1970	1970	510
		(Soluble)	(20)	(80)	(30)
	END-SSP370-BIOF	Total	1970	1970	510
		(Soluble)	(90)	(150)	(50)

616

617

618 Modeled changes in residential coal emissions most impacted global soluble Fe fluxes
619 when compared to other fuel-types, and this was likely attributed to the fact that residential
620 coal Fe emissions (464 Gg a^{-1}) exceeded individual emissions from all other fuel types in our

https://doi.org/10.5194/egusphere-2025-4058
Preprint. Discussion started: 28 August 2025

PD emissions dataset (industrial coal: 305 Gg a^{-1}; oil: 34 Gg a^{-1}; residential biofuel: 72 Gg a^{-1}), with the exception of smelting (1345 Gg a^{-1}). Furthermore, the solubility modification for residential coal exceeded the relative changes to all other sectors (from 0.2% to 33%), resulting in emission increase of soluble Fe by a factor of 10 in some regions (Figure 3).

3.3.2 Model-observation comparisons of total and soluble Fe concentrations

Comparison of modelled surface concentrations with regionally grouped, ship-based observations revealed good agreement between modeled and observed total and soluble aerosol Fe concentrations (Figure 4). Modeled total Fe concentrations fell slightly under observed values but remained well within one order of magnitude for each ocean region, with the exception of the Southern Ocean where total Fe was underestimated by several orders of magnitude. Our underestimation of total aerosol Fe in the Southern Ocean aligns with previous efforts to model global fluxes of total and soluble aerosol Fe using MIMI v1.0 and other Earth System Models (Ito and Miyakawa, 2023; Ito et al., 2019; Liu et al., 2024). Current leading hypotheses suggest that an Fe source, such as volcanism or mining, is not currently well represented in models, or alternatively, that limited observations are not representative of typical Fe conditions in the airshed of the Southern Ocean (Ito and Miyakawa, 2023; Liu et al., 2024).

https://doi.org/10.5194/egusphere-2025-4058
Preprint. Discussion started: 28 August 2025

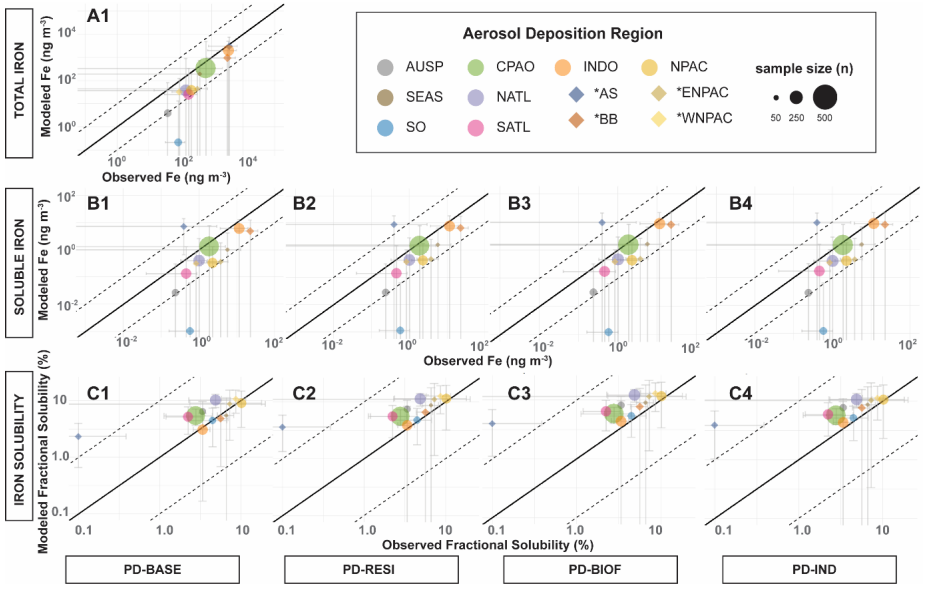

Figure 4. Comparison of modelling and observational data: A) total Fe, B) soluble Fe, and C) Fe solubility; 1) PD-BASE, 2) PD-RESI, 3) PD-BIOF, and 4) PD-IND. Annual averages were aggregated as medians and plotted by deposition region. Error bars represent spatiotemporal variance within each region. The solid black line indicates a 1-to-1 relationship between modeled and observed values and the dashed lines represent deviation by ±1 order of magnitude. Only PD-BASE is shown for total Fe as total Fe fluxes were not manipulated between model cases.

In the PD-BASE case, for soluble Fe concentrations, regression analyses followed a similar trend to total Fe, wherein for each deposition region, modeled averages were slightly lower than observed values and fell within one order of magnitude, except for the Southern Ocean and the Arabian Sea (Figure 4). In the PD-RESI and PD-BIOF cases, average soluble Fe concentrations increased in every ocean region across the globe. At the global scale,

https://doi.org/10.5194/egusphere-2025-4058
Preprint. Discussion started: 28 August 2025

modifications made to anthropogenic Fe solubilities overall lessened the underestimation of soluble Fe by MIMI (Figure 4). Increasing Fe solubility for residential coal burning emission resulted in an average increase to modeled soluble Fe concentrations by 0.5 ± 0.7 ng m^{-3} in each ocean region (Table S8). Conversely, enhancing Fe solubility in residential biofuel burning emission only improved model performance within the South Atlantic Ocean (Figure 4); solubility modifications to fossil fuel sources of Fe (industrial coal and oil emissions) did little to improve model performance (Figure 4). Model performance improvements attributed to soluble Fe in residential coal emissions were especially noticeable for Southeastern Asia, the Bay of Bengal, the North Pacific, and the North Atlantic (Figure 4), likely because of the strong source of residential coal combustion aerosol from China, India, and Europe (Figure 3).

Despite slight underestimations for total and soluble Fe by PD-BASE, Fe solubilities calculated by the model were well aligned with observations for every region except for the Arabian Sea, wherein solubility was overestimated by 1-2 orders of magnitude (Figure 4). In previous MIMI-validation efforts (Hamilton et al., 2019), observational data from the Arabian Sea and Bay of Bengal were aggregated as the Indian Ocean, but each basin has distinct terrestrial sources of aerosol. While both receive a large source of anthropogenic emission from India, the Arabian Sea has a much larger dust influence from the Middle East and the Bay of Bengal is more strongly affected by anthropogenic emissions across Southeastern Asia (Bali et al., 2019; Guieu et al., 2019).

In general, we found that ocean regions which are known to be influenced by dust Fe had slightly higher overestimations for Fe solubility when compared to regions with less dust deposition (Figure 4C). Specifically, Fe solubility in the South Atlantic (heavily influenced by

https://doi.org/10.5194/egusphere-2025-4058
Preprint. Discussion started: 28 August 2025

dust emitted from the Patagonia Desert), the Central Atlantic/Pacific and North Atlantic (Sahara Desert), Australia/South Pacific (Great Victoria Desert), and North Pacific (Gobi Desert), was overestimated when compared to other regions (Figure 4C). These findings suggest that soluble Fe in dust is slightly overrepresented in the current model scheme (Figure 4). However, it is important to highlight that use of the new soil scheme that includes how soil moisture changes impact dust emissions, as revealed herein, indicated an improvement from previous model simulations for dust Fe (Hamilton et al., 2019; Myriokefalitakis et al., 2018).

In regions with less dust Fe and stronger sources of anthropogenic Fe, Fe solubilities were slightly underestimated by the baseline simulation. In each of our modified solubility cases (PD-RESI, PD-BIOF, and PD-IND), Fe solubility for southeastern Asia, the Bay of Bengal, the North Pacific, and the Southern Ocean all increased, but the regions heavily impacted by dust remained relatively unchanged (Figure 4). This suggests that modifications to Fe solubility for anthropogenic combustion aerosol as applied herein improve the predictive capability of MIMI in regions with heavy anthropogenic influence.

3.3.3 Soluble Fe under PI and FU emission scenarios

PI model simulations serve as a valuable baseline in understanding the specific implications of anthropogenic perturbation on the Earth system. When comparing soluble Fe emitted in the PI and PD, we found increases in soluble Fe fluxes for most regions across the globe (Figure 5). Such increases were largely attributed to steadily growing anthropogenic combustion and industrial activity emissions over time. However, dust and wildfire Fe emissions were also distinct between the PI and PD, due to land-use changes and global warming induced feedbacks that have altered global precipitation patterns (Hamilton et al.,

https://doi.org/10.5194/egusphere-2025-4058
Preprint. Discussion started: 28 August 2025

2018; Kok et al., 2023; Li et al., 2019; Mahowald et al., 2010). Globally, we estimated that soluble Fe fluxes to marine ecosystems in the PD exceeded these during the PI era by 36-70 Gg a^{-1}, with the low estimate from PD-BASE and the high estimate from PD-BIOF case. We observed the largest differences between PI and PD soluble Fe fluxes in Southeastern Asia, the Bay of Bengal, and the North Atlantic. These differences were apparent for all the solubility parameterizations used and deposition regions (Figures 5 and S4), apart from the South Atlantic region where soluble Fe fluxes in the PI era exceeded PD fluxes by 5.6 Gg a^{-1}. This decrease was likely attributed to reduction in wildfire burned area over past decades, particularly in Africa (Andela et al., 2017; Jones et al., 2022). Previous work has suggested that wildfire activity during the PI era exceeded current wildfire regimes at the global scale (Hamilton et al., 2018), and our modeling work suggested larger wildfire Fe emission and deposition fluxes in every region during the PI era compared to PD. This signal was also most apparent in the South Atlantic where PD deposition fluxes of wildfire Fe were exceeded by a factor of 4 (Figure 5).

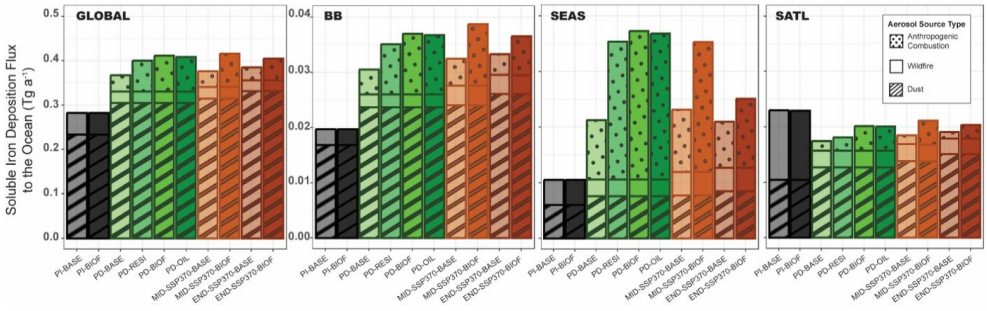

Figure 5. Deposition fluxes of soluble aerosol Fe to marine ecosystems: A) globally; B) Bay of Bengal (BB); C) Southeastern Asia (SEAS); D) South Atlantic (SATL). Deposition fluxes are source-apportioned (dust, wildfire burning, and anthropogenic combustion) and provided for each case with distinct solubility parameters. Plots for each regional grouping (as depicted

https://doi.org/10.5194/egusphere-2025-4058
Preprint. Discussion started: 28 August 2025

in Figure 1) are provided in the supplementary information (Figure S4).

New Fe solubility parameterizations for residential coal emission increased the delivery of anthropogenic soluble aerosol Fe to marine ecosystems by a factor of 1.7 – 2.8 at the regional scale (Figures 3 and 5). Increased fluxes were greatest for Australia/the Southern Pacific, the Southern Atlantic, across Southeastern Asia, the Bay of Bengal, and the Southern Ocean. While model performance showed the most significant improvement in the Bay of Bengal, enhancements in other regions were generally modest, and changes in the Southern Ocean were indiscernible (Figure 4). These regional discrepancies highlight the current limitations of ship-based observations in capturing representative soluble Fe fluxes, particularly in the under-sampled Southern Hemisphere. Future efforts should prioritize expanding the spatial coverage of measurements in these regions to improve model accuracy and understanding of possible anthropogenic influence on remote marine biogeochemistry.

Under the SSP370 future emissions scenario, anthropogenic Fe emissions are projected to reach their maxima by 2050 for most deposition regions and then decrease to values at or below current PD conditions by 2100 (Figure 5). However, this trend did not hold for the global south (Australia/South Pacific, Central Pacific/Atlantic, and Southern Ocean) where soluble aerosol Fe fluxes were projected to continually increase through the end of the century (Figure 5); this was not due to anthropogenic combustion emissions directly, but rather because of dust as the primary source of soluble Fe to the Southern Hemisphere (Figure 5).

By the end of the century under SSP370, model simulations suggested that soluble Fe deposition to marine systems will decrease by a factor of 0.2-0.4 globally, compared to the

https://doi.org/10.5194/egusphere-2025-4058
Preprint. Discussion started: 28 August 2025

present day. In our base simulation (PD-BASE), losses of soluble Fe are projected to be 7 Gg a^{-1} by the year 2100. However, in each of our test cases, the projected changes to soluble Fe fluxes between PD/MID-SSP370 and MID-SSP370/END-SSP370 was more drastic, with midcentury soluble Fe fluxes increasing by 6 Gg a^{-1} by 2050 but falling by up to 32 Gg a^{-1} by the year 2100 (Figure 5). Therefore, marine ecosystems could face a more significant deviation from current soluble Fe supplies than has been previously represented in Earth System Models, and this could largely be attributed to changes in residential sources of combustion aerosol.

At the regional scale, the largest changes to soluble Fe fluxes under SSP370 are anticipated in the Bay of Bengal, the North Atlantic, the South Atlantic, and across Southeastern Asia (Figures 5 and S4). Notably, in Southeastern Asia, anthropogenic combustion exceeded both dust and wildfire Fe, constituting up to 72% of all soluble Fe fluxes to marine ecosystems in this region. By 2100, soluble Fe fluxes were projected to decrease by a factor of 0.2 in the base case (PD-BASE vs. END-SSP370-BASE; Figure 5). However, in the -BIOF cases for these scenarios, fluxes decreased by a factor of 0.5, more than doubling the projected reduction in soluble Fe fluxes. This would constitute a much larger disruption to current biogeochemistry and external sources of Fe in key open ocean regions.

Projected losses in soluble Fe fluxes by 2100 under future emission scenarios, including SSP370, have strong implications for the spatiotemporal distribution of net marine primary productivity, especially in Fe limited regions. Recent work suggested that the atmospheric supply of anthropogenic Fe has already shifted phytoplankton bloom dynamics in the open ocean by accelerating the seasonal uptake of upwelled nitrogen in HNLC regions, such as the North Pacific (Hawco et al., 2025). Such HNLC regions are anticipated to be especially

https://doi.org/10.5194/egusphere-2025-4058
Preprint. Discussion started: 28 August 2025

sensitive to changes in anthropogenic Fe given that they are historically limited by trace metals including Fe (Bazzani et al., 2023; Moore et al., 2013; Nishioka and Obata, 2017).

Diverse lines of evidence suggest that half of the soluble Fe flux to the North Pacific comes from Asian anthropogenic sources (Hamilton et al., 2019; Hamilton et al., 2020b; Hawco et al., 2025; Rathod et al., 2020). Li et al. (2024) found that the magnitude of chlorophyll-a response to Fe deposition off the coast of China was lowered by a factor of 4 during COVID-19 in March 2020 when anthropogenic emissions across East Asia were substantially reduced. The authors speculated that a reduction in soluble Fe from anthropogenic activities, either via the primary emission of soluble Fe or via a reduction in Fe solubilization via co-emitted acidic species (e.g., SO_x), resulted in a lessened supply of soluble Fe delivered during the deposition event. Moreover, using Fe isotopes to trace source origins of atmospheric Fe, Hawco et al. (2025) recently showed that the springtime delivery of anthropogenic Fe could be one major factor driving observed seasonal and geographic shifts to the North Pacific transition zone, a highly productive boundary in the North Pacific. In particular, our findings suggest that residential coal burning is an especially important source of soluble Fe to the North Pacific and the South China Sea, and across southeastern Asia. Accordingly, we find that projected losses of anthropogenic emissions over the course of this century will greatly influence nutrient dynamics in these key marine ecosystems.

4 Conclusions

Anthropogenic activity has added a multitude of new aerosol Fe sources to the atmosphere. Understanding how these new sources alter soluble Fe fluxes aids better understanding of changes to marine primary productivity and ocean ecosystems within the Anthropocene.

https://doi.org/10.5194/egusphere-2025-4058
Preprint. Discussion started: 28 August 2025

However, estimating the contribution of anthropogenic emissions to soluble aerosol Fe fluxes is challenging given the wide variety of sources, leading to large variation across different modeling studies on the magnitude of the deposition fluxes. By measuring Fe content and solubility of aerosol Fe from several important anthropogenic sources and including a first assessment of the contribution from biofuels, we find that median Fe solubilities vary by greater than three order of magnitude, from 0.03% for power plant coal fly ash to 55.87% for biofuel burning aerosol.

To understand the impact of increasing source representation of fractional Fe solubilities measured in this work, we refined Fe solubility parameters within an atmospheric Fe module (MIMI) embedded within the CESM2. We found that current (PD) and projected (FU) fluxes of soluble aerosol Fe to global marine ecosystems could exceed current modeled values by up to a factor of 2, mainly driven by the new addition of a highly soluble biofuel Fe source, highlighting residential burning as a significant source of soluble Fe to the ocean. The most notable impacts were found in the Bay of Bengal, across Southeast Asia, and throughout the North Pacific and North Atlantic (i.e., regions strongly influenced by nearby continental anthropogenic activity). However, many shipborne observations of aerosol Fe have historically been taken in regions outside of biofuel rich Fe plumes, limiting current capacity to constrain model fluxes and highlighting a future research opportunity.

Data availability.

Experimental data can be found in the manuscript or the supplement. Modeling output data, coding scripts, and emission inventories are available at:

https://doi.org/10.5194/egusphere-2025-4058
Preprint. Discussion started: 28 August 2025

https://github.com/haleyplaas/CombustionFe.

Competing interests.

At least one of the (co-)authors is a member of the editorial board of Atmospheric Chemistry and Physics.

Author contribution.

MT initiated this study; MT and DSH designed this study and secured funding resources; RL, YZ, YC and TZ conducted experimental work; HEP, SR and DSH conducted modeling work; YY provided key samples used in this work and contributed to data analysis; RL and HEP analyzed the results; RL, HEP, DSH and MT wrote the manuscript; all the authors reviewed and approved the manuscript.

Financial support.

This work was sponsored by National Natural Science Foundation of China (42321003, 42277088 and 22361162668), International Partnership Program of Chinese Academy of Sciences (164GJHZ2024011FN), Guangzhou Bureau of Science and Technology (2024A04J6533), and Guangdong Foundation for the Program of Science and Technology Research (2023B1212060049).

https://doi.org/10.5194/egusphere-2025-4058
Preprint. Discussion started: 28 August 2025

References

Agrawal, H., Malloy, Q. G. J., Welch, W. A., Wayne Miller, J., and Cocker, D. R.: In-use gaseous and particulate matter emissions from a modern ocean going container vessel, Atmospheric Environment, 42, 5504-5510, https://doi.org/10.1016/j.atmosenv.2008.02.053, 2008.

Ahmaruzzaman, M.: A review on the utilization of fly ash, Progress in Energy and Combustion Science, 36, 327-363, https://doi.org/10.1016/j.pecs.2009.11.003, 2010.

Al-Abadleh, H. A., Kubicki, J. D., and Meskhidze, N.: A perspective on iron (Fe) in the atmosphere: air quality, climate, and the ocean, Environmental Science: Processes & Impacts, 25, 151-164, 10.1039/D2EM00176D, 2023.

Al-Negheimish, A. I., Al-Mutlaq, F. M., Fares, G., Alhozaimy, A. M., and Iqbal Khan, M.: Characterization of chemical accelerators for sustainable recycling of fresh electric-arc furnace dust in cement pastes, Advanced Powder Technology, 32, 3046-3062, https://doi.org/10.1016/j.apt.2021.06.019, 2021.

Alizadeh, M., and Momeni, M.: The effect of the scrap/DRI ratio on the specification of the EAF dust and its influence on mechanical properties of the concrete treated by its dust, Construction and Building Materials, 112, 1041-1045, https://doi.org/10.1016/j.conbuildmat.2016.03.011, 2016.

Alsheyab, M. A. T., and Khedaywi, T. S.: Analysis of the Effect of Temperature on the Resilient Modulus of Asphalt Concrete Mixed with Electric Arc Furnace Dust (EAFD), Water, Air, & Soil Pollution, 227, 80, 10.1007/s11270-016-2776-4, 2016.

Alves, C., Gonçalves, C., Fernandes, A. P., Tarelho, L., and Pio, C.: Fireplace and woodstove fine particle emissions from combustion of western Mediterranean wood types, Atmospheric Research, 101, 692-700, https://doi.org/10.1016/j.atmosres.2011.04.015, 2011.

Andela, N., Morton, D. C., Giglio, L., Chen, Y., van der Werf, G. R., Kasibhatla, P. S., DeFries, R. S., Collatz, G. J., Hantson, S., Kloster, S., Bachelet, D., Forrest, M., Lasslop, G., Li, F., Mangeon, S., Melton, J. R., Yue, C., and Randerson, J. T.: A human-driven decline in global burned area, Science, 356, 1356-1362, 10.1126/science.aal4108, 2017.

Baker, A. R., Li, M., and Chance, R.: Trace Metal Fractional Solubility in Size-Segregated Aerosols From the Tropical Eastern Atlantic Ocean, Global Biogeochemical Cycles, 34, e2019GB006510, https://doi.org/10.1029/2019GB006510, 2020.

Baldo, C., Ito, A., Krom, M. D., Li, W., Jones, T., Drake, N., Ignatyev, K., Davidson, N., and Shi, Z.: Iron from coal combustion particles dissolves much faster than mineral dust under simulated atmospheric acidic conditions, Atmospheric Chemistry and Physics, 22, 6045-6066, 10.5194/acp-22-6045-2022, 2022.

Bali, K., Mishra, A. K., Singh, S., Chandra, S., and Lehahn, Y.: Impact of dust storm on phytoplankton bloom over the Arabian Sea: a case study during March 2012, Environ Sci Pollut Res Int, 26, 11940-11950, 10.1007/s11356-019-04602-7, 2019.

Bayuseno, A. P., and Schmahl, W. W.: Characterization of MSWI fly ash through mineralogy and water extraction, Resources, Conservation and Recycling, 55, 524-534, https://doi.org/10.1016/j.resconrec.2011.01.002, 2011.

Bazzani, E., Lauritano, C., and Saggiomo, M.: Southern Ocean Iron Limitation of Primary Production between Past Knowledge and Future Projections, Journal of Marine Science and Engineering, 11, 272, https://doi.org/10.3390/jmse11020272, 2023.

Bergas-Massó, E., Gonçalves Ageitos, M., Myriokefalitakis, S., Miller, R. L., van Noije, T., Le Sager, P., Montané Pinto, G., and Pérez García-Pando, C.: Pre-Industrial, Present and Future Atmospheric Soluble Iron Deposition and the Role of Aerosol Acidity and Oxalate Under CMIP6 Emissions, Earth's Future, 11, e2022EF003353, https://doi.org/10.1029/2022EF003353, 2023.

https://doi.org/10.5194/egusphere-2025-4058
Preprint. Discussion started: 28 August 2025

Bergas-Masso, E., Hamilton, D. S., Myriokefalitakis, S., Rathod, S., Gonçalves Ageitos, M., and Pérez García-Pando, C.: Future climate-driven fires may boost ocean productivity in the iron-limited North Atlantic, Nature Climate Change, 15, 784-792, 10.1038/s41558-025-02356-4, 2025.

Bhargava, S. K., Garg, A., and Subasinghe, N. D.: In situ high-temperature phase transformation studies on pyrite, Fuel, 88, 988-993, https://doi.org/10.1016/j.fuel.2008.12.005, 2009.

Blissett, R. S., and Rowson, N. A.: A review of the multi-component utilisation of coal fly ash, Fuel, 97, 1-23, https://doi.org/10.1016/j.fuel.2012.03.024, 2012.

Bond, T. C., Streets, D. G., Yarber, K. F., Nelson, S. M., Woo, J.-H., and Klimont, Z.: A technology-based global inventory of black and organic carbon emissions from combustion, Journal of Geophysical Research: Atmospheres, 109, https://doi.org/10.1029/2003JD003697, 2004.

Bond, T. C., Bhardwaj, E., Dong, R., Jogani, R., Jung, S., Roden, C., Streets, D. G., and Trautmann, N. M.: Historical emissions of black and organic carbon aerosol from energy-related combustion, 1850–2000, Global Biogeochemical Cycles, 21, https://doi.org/10.1029/2006GB002840, 2007.

Celo, V., Dabek-Zlotorzynska, E., and McCurdy, M.: Chemical Characterization of Exhaust Emissions from Selected Canadian Marine Vessels: The Case of Trace Metals and Lanthanoids, Environmental Science & Technology, 49, 5220-5226, 10.1021/acs.est.5b00127, 2015.

Chen, H., Laskin, A., Baltrusaitis, J., Gorski, C. A., Scherer, M. M., and Grassian, V. H.: Coal Fly Ash as a Source of Iron in Atmospheric Dust, Environmental Science & Technology, 46, 2112-2120, 10.1021/es204102f, 2012.

Chen, Y., Wang, Z., Fang, Z., Huang, C., Xu, H., Zhang, H., Zhang, T., Wang, F., Luo, L., Shi, G., Wang, X., and Tang, M.: Dominant Contribution of Non-dust Primary Emissions and Secondary Processes to Dissolved Aerosol Iron, Environmental Science & Technology, 58, 17355-17363, 10.1021/acs.est.4c05816, 2024.

Chuang, P. Y., Duvall, R. M., Shafer, M. M., and Schauer, J. J.: The origin of water soluble particulate iron in the Asian atmospheric outflow, Geophysical Research Letters, 32, 4, 10.1029/2004gl021946, 2005.

Cobo, M., Gálvez, A., Conesa, J. A., and Montes de Correa, C.: Characterization of fly ash from a hazardous waste incinerator in Medellin, Colombia, Journal of Hazardous Materials, 168, 1223-1232, https://doi.org/10.1016/j.jhazmat.2009.02.169, 2009.

Danabasoglu, G., Lamarque, J. F., Bacmeister, J., Bailey, D. A., DuVivier, A. K., Edwards, J., Emmons, L. K., Fasullo, J., Garcia, R., Gettelman, A., Hannay, C., Holland, M. M., Large, W. G., Lauritzen, P. H., Lawrence, D. M., Lenaerts, J. T. M., Lindsay, K., Lipscomb, W. H., Mills, M. J., Neale, R., Oleson, K. W., Otto-Bliesner, B., Phillips, A. S., Sacks, W., Tilmes, S., van Kampenhout, L., Vertenstein, M., Bertini, A., Dennis, J., Deser, C., Fischer, C., Fox-Kemper, B., Kay, J. E., Kinnison, D., Kushner, P. J., Larson, V. E., Long, M. C., Mickelson, S., Moore, J. K., Nienhouse, E., Polvani, L., Rasch, P. J., and Strand, W. G.: The Community Earth System Model Version 2 (CESM2), Journal of Advances in Modeling Earth Systems, 12, e2019MS001916, https://doi.org/10.1029/2019MS001916, 2020.

Deng, J., Ma, X., Zhang, Y., Li, Y., and Zhu, W.: Effects of pyrite on the spontaneous combustion of coal, International Journal of Coal Science & Technology, 2, 306-311, 10.1007/s40789-015-0085-y, 2015.

Desboeufs, K. V., Sofikitis, A., Losno, R., Colin, J. L., and Ausset, P.: Dissolution and solubility of trace metals from natural and anthropogenic aerosol particulate matter, Chemosphere, 58, 195-203, https://doi.org/10.1016/j.chemosphere.2004.02.025, 2005.

Dutta, B. K., Khanra, S., and Mallick, D.: Leaching of elements from coal fly ash: Assessment of its potential for use in filling abandoned coal mines, Fuel, 88, 1314-1323, https://doi.org/10.1016/j.fuel.2009.01.005, 2009.

Fu, H., Lin, J., Shang, G., Dong, W., Grassian, V. H., Carmichael, G. R., Li, Y., and Chen, J.: Solubility of Iron from Combustion Source Particles in Acidic Media Linked to Iron Speciation, Environmental Science & Technology, 46, 11119-11127, 10.1021/es302558m, 2012.

https://doi.org/10.5194/egusphere-2025-4058
Preprint. Discussion started: 28 August 2025

907 Funari, V., Mäkinen, J., Salminen, J., Braga, R., Dinelli, E., and Revitzer, H.: Metal removal from Municipal Solid
908 Waste Incineration fly ash: A comparison between chemical leaching and bioleaching, Waste Management,
909 60, 397-406, https://doi.org/10.1016/j.wasman.2016.07.025, 2017.
910 García-López, N., Ingabire, A. S., Bailis, R., Eriksson, A. C., Isaxon, C., and Boman, C.: Biomass cookstove
911 emissions—a systematic review on aerosol and particle properties of relevance for health, climate, and the
912 environment, Environmental Research Letters, 20, 053002, 10.1088/1748-9326/adc615, 2025.
913 Goncalves, C., Alves, C., Evtyugina, M., Mirante, F., Pio, C., Caseiro, A., Schmidl, C., Bauer, H., and Carvalho,
914 F.: Characterisation of PM10 emissions from woodstove combustion of common woods grown in Portugal,
915 Atmospheric Environment, 44, 4474-4480, https://doi.org/10.1016/j.atmosenv.2010.07.026, 2010.
916 Goodarzi, F.: Characteristics and composition of fly ash from Canadian coal-fired power plants, Fuel, 85, 1418-
917 1427, https://doi.org/10.1016/j.fuel.2005.11.022, 2006.
918 Guieu, C., Al Azhar, M., Aumont, O., Mahowald, N., Levy, M., Ethé, C., and Lachkar, Z.: Major Impact of Dust
919 Deposition on the Productivity of the Arabian Sea, Geophysical Research Letters, 46, 6736-6744,
920 https://doi.org/10.1029/2019GL082770, 2019.
921 Hamilton, D., Kasoar, M., Bergas-Massó, E., Dalmonech, D., Hantson, S., Lasslop, G., Voulgarakis, A., and Wells,
922 C.: Global Warming Increases Fire Emissions but Resulting Aerosol Forcing is Uncertain, 10.21203/rs.3.rs-
923 4567012/v1, 2024.
924 Hamilton, D. S., Hantson, S., Scott, C. E., Kaplan, J. O., Pringle, K. J., Nieradzik, L. P., Rap, A., Folberth, G. A.,
925 Spracklen, D. V., and Carslaw, K. S.: Reassessment of pre-industrial fire emissions strongly affects
926 anthropogenic aerosol forcing, Nature Communications, 9, 3182, 10.1038/s41467-018-05592-9, 2018.
927 Hamilton, D. S., Scanza, R. A., Feng, Y., Guinness, J., Kok, J. F., Li, L., Liu, X., Rathod, S. D., Wan, J. S., Wu,
928 M., and Mahowald, N. M.: Improved methodologies for Earth system modelling of atmospheric soluble iron
929 and observation comparisons using the Mechanism of Intermediate complexity for Modelling Iron (MIMI
930 v1.0), Geoscientific Model Development, 12, 3835-3862, 10.5194/gmd-12-3835-2019, 2019.
931 Hamilton, D. S., Moore, J. K., Arneth, A., Bond, T. C., Carslaw, K. S., Hantson, S., Ito, A., Kaplan, J. O., Lindsay,
932 K., Nieradzik, L., Rathod, S. D., Scanza, R. A., and Mahowald, N. M.: Impact of Changes to the Atmospheric
933 Soluble Iron Deposition Flux on Ocean Biogeochemical Cycles in the Anthropocene, Global Biogeochemical
934 Cycles, 34, e2019GB006448, https://doi.org/10.1029/2019GB006448, 2020a.
935 Hamilton, D. S., Scanza, R. A., Rathod, S. D., Bond, T. C., Kok, J. F., Li, L., Matsui, H., and Mahowald, N. M.:
936 Recent (1980 to 2015) Trends and Variability in Daily-to-Interannual Soluble Iron Deposition from Dust, Fire,
937 and Anthropogenic Sources, Geophysical Research Letters, 47, e2020GL089688,
938 https://doi.org/10.1029/2020GL089688, 2020b.
939 Hamilton, D. S., Perron, M. M. G., Bond, T. C., Bowie, A. R., Buchholz, R. R., Guieu, C., Ito, A., Maenhaut, W.,
940 Myriokefalitakis, S., Olgun, N., Rathod, S. D., Schepanski, K., Tagliabue, A., Wagner, R., and Mahowald, N.
941 M.: Earth, Wind, Fire, and Pollution: Aerosol Nutrient Sources and Impacts on Ocean Biogeochemistry,
942 Annual Review of Marine Science, 14, 303-330, 10.1146/annurev-marine-031921-013612, 2022.
943 Hamilton, D. S., Baker, A. R., Iwamoto, Y., Gassó, S., Bergas-Masso, E., Deutch, S., Dinasquet, J., Kondo, Y.,
944 Llort, J., Myriokefalitakis, S., Perron, M. M. G., Wegmann, A., and Yoon, J.-E.: An aerosol odyssey:
945 Navigating nutrient flux changes to marine ecosystems, Elementa: Science of the Anthropocene, 11, 00037,
946 10.1525/elementa.2023.00037, 2023.
947 Hawco, N. J., Conway, T. M., Coesel, S. N., Barone, B., Seelen, E. A., Yang, S.-C., Bundy, R. M., Pinedo-Gonzalez,
948 P., Bian, X., Sieber, M., Lanning, N. T., Fitzsimmons, J. N., Foreman, R. K., König, D., Groussman, M. J.,
949 Allen, J. G., Juranek, L. W., White, A. E., Karl, D. M., Armbrust, E. V., and John, S. G.: Anthropogenic iron
950 alters the spring phytoplankton bloom in the North Pacific transition zone, Proceedings of the National

https://doi.org/10.5194/egusphere-2025-4058
Preprint. Discussion started: 28 August 2025

Academy of Sciences, 122, e2418201122, 10.1073/pnas.2418201122, 2025.

Hedberg, E., Kristensson, A., Ohlsson, M., Johansson, C., Johansson, P.-Å., Swietlicki, E., Vesely, V., Wideqvist, U., and Westerholm, R.: Chemical and physical characterization of emissions from birch wood combustion in a wood stove, Atmospheric Environment, 36, 4823-4837, https://doi.org/10.1016/S1352-2310(02)00417-X, 2002.

Hildemann, L. M., Markowski, G. R., and Cass, G. R.: Chemical composition of emissions from urban sources of fine organic aerosol, Environmental Science & Technology, 25, 744-759, 10.1021/es00016a021, 1991.

Hoesly, R. M., Smith, S. J., Feng, L., Klimont, Z., Janssens-Maenhout, G., Pitkanen, T., Seibert, J. J., Vu, L., Andres, R. J., Bolt, R. M., Bond, T. C., Dawidowski, L., Kholod, N., Kurokawa, J. I., Li, M., Liu, L., Lu, Z., Moura, M. C. P., O'Rourke, P. R., and Zhang, Q.: Historical (1750–2014) anthropogenic emissions of reactive gases and aerosols from the Community Emissions Data System (CEDS), Geoscientific Model Development, 11, 369-408, 10.5194/gmd-11-369-2018, 2018.

Hu, G., Dam-Johansen, K., Wedel, S., and Hansen, J. P.: Decomposition and oxidation of pyrite, Progress in Energy and Combustion Science, 32, 295-314, https://doi.org/10.1016/j.pecs.2005.11.004, 2006.

Itahashi, S., Hattori, S., Ito, A., Sadanaga, Y., Yoshida, N., and Matsuki, A.: Role of Dust and Iron Solubility in Sulfate Formation during the Long-Range Transport in East Asia Evidenced by 17O-Excess Signatures, Environmental Science & Technology, 56, 13634-13643, 10.1021/acs.est.2c03574, 2022.

Ito, A., and Shi, Z.: Delivery of anthropogenic bioavailable iron from mineral dust and combustion aerosols to the ocean, Atmospheric Chemistry and Physics, 16, 85-99, 10.5194/acp-16-85-2016, 2016.

Ito, A., Lin, G., and Penner, J. E.: Radiative forcing by light-absorbing aerosols of pyrogenetic iron oxides, Scientific Reports, 8, 7347, 10.1038/s41598-018-25756-3, 2018.

Ito, A., Myriokefalitakis, S., Kanakidou, M., Mahowald, N. M., Scanza, R. A., Hamilton, D. S., Baker, A. R., Jickells, T., Sarin, M., Bikkina, S., Gao, Y., Shelley, R. U., Buck, C. S., Landing, W. M., Bowie, A. R., Perron, M. M. G., Guieu, C., Meskhidze, N., Johnson, M. S., Feng, Y., Kok, J. F., Nenes, A., and Duce, R. A.: Pyrogenic iron: The missing link to high iron solubility in aerosols, Science Advances, 5, 10, 10.1126/sciadv.aau7671, 2019.

Ito, A., Ye, Y., Baldo, C., and Shi, Z.: Ocean fertilization by pyrogenic aerosol iron, npj Climate and Atmospheric Science, 4, 30, 10.1038/s41612-021-00185-8, 2021.

Ito, A., and Miyakawa, T.: Aerosol Iron from Metal Production as a Secondary Source of Bioaccessible Iron, Environmental Science & Technology, 57, 4091-4100, 10.1021/acs.est.2c06472, 2023.

Jahn, L. G., Jahl, L. G., Bland, G. D., Bowers, B. B., Monroe, L. W., and Sullivan, R. C.: Metallic and Crustal Elements in Biomass-Burning Aerosol and Ash: Prevalence, Significance, and Similarity to Soil Particles, Acs Earth and Space Chemistry, 5, 136-148, 10.1021/acsearthspacechem.0c00191, 2021.

Jankowski, J., Ward, C. R., French, D., and Groves, S.: Mobility of trace elements from selected Australian fly ashes and its potential impact on aquatic ecosystems, Fuel, 85, 243-256, https://doi.org/10.1016/j.fuel.2005.05.028, 2006.

Johnson, M. S., and Meskhidze, N.: Atmospheric dissolved iron deposition to the global oceans: effects of oxalate-promoted Fe dissolution, photochemical redox cycling, and dust mineralogy, Geoscientific Model Development, 6, 1137-1155, 10.5194/gmd-6-1137-2013, 2013.

Jones, M. W., Abatzoglou, J. T., Veraverbeke, S., Andela, N., Lasslop, G., Forkel, M., Smith, A. J. P., Burton, C., Betts, R. A., van der Werf, G. R., Sitch, S., Canadell, J. G., Santín, C., Kolden, C., Doerr, S. H., and Le Quéré, C.: Global and Regional Trends and Drivers of Fire Under Climate Change, Reviews of Geophysics, 60, e2020RG000726, https://doi.org/10.1029/2020RG000726, 2022.

Journet, E., Desboeufs, K. V., Caquineau, S., and Colin, J.-L.: Mineralogy as a critical factor of dust iron solubility,

https://doi.org/10.5194/egusphere-2025-4058
Preprint. Discussion started: 28 August 2025

Geophysical Research Letters, 35, 10.1029/2007gl031589, 2008.
Knorr, W., Jiang, L., and Arneth, A.: Climate, CO2 and human population impacts on global wildfire emissions, Biogeosciences, 13, 267-282, 10.5194/bg-13-267-2016, 2016.
Kok, J. F., Storelvmo, T., Karydis, V. A., Adebiyi, A. A., Mahowald, N. M., Evan, A. T., He, C., and Leung, D. M.: Mineral dust aerosol impacts on global climate and climate change, Nature Reviews Earth & Environment, 4, 71-86, 10.1038/s43017-022-00379-5, 2023.
Kutchko, B. G., and Kim, A. G.: Fly ash characterization by SEM–EDS, Fuel, 85, 2537-2544, https://doi.org/10.1016/j.fuel.2006.05.016, 2006.
Laforest, G., and Duchesne, J.: Stabilization of electric arc furnace dust by the use of cementitious materials: Ionic competition and long-term leachability, Cement and Concrete Research, 36, 1628-1634, https://doi.org/10.1016/j.cemconres.2006.05.012, 2006.
Li, C., Liu, W., Jiao, F., Yang, C., Li, G., Liu, S., and Qin, W.: Separation and recovery of zinc, lead and iron from electric arc furnace dust by low temperature smelting, Separation and Purification Technology, 312, 123355, https://doi.org/10.1016/j.seppur.2023.123355, 2023.
Li, F., Val Martin, M., Andreae, M. O., Arneth, A., Hantson, S., Kaiser, J. W., Lasslop, G., Yue, C., Bachelet, D., Forrest, M., Kluzek, E., Liu, X., Mangeon, S., Melton, J. R., Ward, D. S., Darmenov, A., Hickler, T., Ichoku, C., Magi, B. I., Sitch, S., van der Werf, G. R., Wiedinmyer, C., and Rabin, S. S.: Historical (1700–2012) global multi-model estimates of the fire emissions from the Fire Modeling Intercomparison Project (FireMIP), Atmospheric Chemistry and Physics, 19, 12545-12567, 10.5194/acp-19-12545-2019, 2019.
Li, L., Mahowald, N. M., Kok, J. F., Liu, X., Wu, M., Leung, D. M., Hamilton, D. S., Emmons, L. K., Huang, Y., Sexton, N., Meng, J., and Wan, J.: Importance of different parameterization changes for the updated dust cycle modeling in the Community Atmosphere Model (version 6.1), Geoscientific Model Development, 15, 8181-8219, 10.5194/gmd-15-8181-2022, 2022a.
Li, R., Zhang, H., Wang, F., He, Y., Huang, C., Luo, L., Dong, S., Jia, X., and Tang, M.: Mass fractions, solubility, speciation and isotopic compositions of iron in coal and municipal waste fly ash, Science of The Total Environment, 838, 155974, https://doi.org/10.1016/j.scitotenv.2022.155974, 2022b.
Li, R., Zhang, H., Wang, F., Ren, Y., Jia, S., Jiang, B., Jia, X., Tang, Y., and Tang, M.: Abundance and fractional solubility of phosphorus and trace metals in combustion ash and desert dust: Implications for bioavailability and reactivity, Science of The Total Environment, 816, 151495, https://doi.org/10.1016/j.scitotenv.2021.151495, 2022c.
Li, S., Zhang, B., Wu, D., Li, Z., Chu, S.-Q., Ding, X., Tang, X., Chen, J., and Li, Q.: Magnetic Particles Unintentionally Emitted from Anthropogenic Sources: Iron and Steel Plants, Environmental Science & Technology Letters, 8, 295-300, 10.1021/acs.estlett.1c00164, 2021.
Li, W., Xu, L., Liu, X., Zhang, J., Lin, Y., Yao, X., Gao, H., Zhang, D., Chen, J., Wang, W., Harrison, R. M., Zhang, X., Shao, L., Fu, P., Nenes, A., and Shi, Z.: Air pollution–aerosol interactions produce more bioavailable iron for ocean ecosystems, Science Advances, 3, e1601749, 10.1126/sciadv.1601749, 2017.
Li, Y., Wang, W., Han, Y., Liu, W., Wang, R., Zhang, R., Zhao, Z., Sheng, L., and Zhou, Y.: Impact of COVID-19 emission reduction on dust aerosols and marine chlorophyll-a concentration, Science of The Total Environment, 918, 170493, https://doi.org/10.1016/j.scitotenv.2024.170493, 2024.
Lin, K. L., Wang, K. S., Tzeng, B. Y., and Lin, C. Y.: The reuse of municipal solid waste incinerator fly ash slag as a cement substitute, Resources, Conservation and Recycling, 39, 315-324, https://doi.org/10.1016/S0921-3449(02)00172-6, 2003.
Liu, C., Han, G., Hu, B., Geng, F., Liu, M., Dai, S., and Yang, Y.: Fast Screening of Coal Fly Ash with Potential for Rare Earth Element Recovery by Electron Paramagnetic Resonance Spectroscopy, Environmental Science

https://doi.org/10.5194/egusphere-2025-4058
Preprint. Discussion started: 28 August 2025

& Technology, 55, 16716-16722, 10.1021/acs.est.1c06658, 2021.
Liu, L., Li, W., Lin, Q., Wang, Y., Zhang, J., Zhu, Y., Yuan, Q., Zhou, S., Zhang, D., Baldo, C., and Shi, Z.: Size-dependent aerosol iron solubility in an urban atmosphere, npj Climate and Atmospheric Science, 5, 53, 10.1038/s41612-022-00277-z, 2022.
Liu, M., Matsui, H., Hamilton, D. S., Rathod, S. D., Lamb, K. D., and Mahowald, N. M.: Representation of iron aerosol size distributions of anthropogenic emissions is critical in evaluating atmospheric soluble iron input to the ocean, Atmospheric Chemistry and Physics, 24, 13115-13127, 10.5194/acp-24-13115-2024, 2024.
Liu, Y., Zheng, L., Li, X., and Xie, S.: SEM/EDS and XRD characterization of raw and washed MSWI fly ash sintered at different temperatures, J Hazard Mater, 162, 161-173, https://doi.org/10.1016/j.jhazmat.2008.05.029, 2009.
Loaiza, A., Cifuentes, S., and Colorado, H. A.: Asphalt modified with superfine electric arc furnace steel dust (EAF dust) with high zinc oxide content, Construction and Building Materials, 145, 538-547, https://doi.org/10.1016/j.conbuildmat.2017.04.050, 2017.
Longo, A. F., Feng, Y., Lai, B., Landing, W. M., Shelley, R. U., Nenes, A., Mihalopoulos, N., Violaki, K., and Ingall, E. D.: Influence of Atmospheric Processes on the Solubility and Composition of Iron in Saharan Dust, Environmental Science & Technology, 50, 6912-6920, 10.1021/acs.est.6b02605, 2016.
Luo, C., Mahowald, N., Bond, T., Chuang, P. Y., Artaxo, P., Siefert, R., Chen, Y., and Schauer, J.: Combustion iron distribution and deposition, Global Biogeochemical Cycles, 22, 10.1029/2007GB002964, 2008.
Machado, J. G. M. S., Brehm, F. A., Moraes, C. A. M., Santos, C. A. d., Vilela, A. C. F., and Cunha, J. B. M. d.: Chemical, physical, structural and morphological characterization of the electric arc furnace dust, J Hazard Mater, 136, 953-960, https://doi.org/10.1016/j.jhazmat.2006.01.044, 2006.
Mahowald, N. M., Engelstaedter, S., Luo, C., Sealy, A., Artaxo, P., Benitez-Nelson, C., Bonnet, S., Chen, Y., Chuang, P. Y., Cohen, D. D., Dulac, F., Herut, B., Johansen, A. M., Kubilay, N., Losno, R., Maenhaut, W., Paytan, A., Prospero, J. M., Shank, L. M., and Siefert, R. L.: Atmospheric Iron Deposition: Global Distribution, Variability, and Human Perturbations*, Annual Review of Marine Science, 1, 245-278, https://doi.org/10.1146/annurev.marine.010908.163727, 2009.
Mahowald, N. M., Kloster, S., Engelstaedter, S., Moore, J. K., Mukhopadhyay, S., McConnell, J. R., Albani, S., Doney, S. C., Bhattacharya, A., Curran, M. A. J., Flanner, M. G., Hoffman, F. M., Lawrence, D. M., Lindsay, K., Mayewski, P. A., Neff, J., Rothenberg, D., Thomas, E., Thornton, P. E., and Zender, C. S.: Observed 20th century desert dust variability: impact on climate and biogeochemistry, Atmospheric Chemistry and Physics, 10, 10875-10893, 10.5194/acp-10-10875-2010, 2010.
Mahowald, N. M., Hamilton, D. S., Mackey, K. R. M., Moore, J. K., Baker, A. R., Scanza, R. A., and Zhang, Y.: Aerosol trace metal leaching and impacts on marine microorganisms, Nature Communications, 9, 2614, 10.1038/s41467-018-04970-7, 2018.
Matsui, H., Mahowald, N. M., Moteki, N., Hamilton, D. S., Ohata, S., Yoshida, A., Koike, M., Scanza, R. A., and Flanner, M. G.: Anthropogenic combustion iron as a complex climate forcer, Nature Communications, 9, 1593, 10.1038/s41467-018-03997-0, 2018.
McDaniel, M. F. M., Ingall, E. D., Morton, P. L., Castorina, E., Weber, R. J., Shelley, R. U., Landing, W. M., Longo, A. F., Feng, Y., and Lai, B.: Relationship between Atmospheric Aerosol Mineral Surface Area and Iron Solubility, Acs Earth and Space Chemistry, 3, 2443-2451, 10.1021/acsearthspacechem.9b00152, 2019.
Meij, R.: Trace element behavior in coal-fired power plants, Fuel Processing Technology, 39, 199-217, https://doi.org/10.1016/0378-3820(94)90180-5, 1994.
Moore, C. M., Mills, M. M., Arrigo, K. R., Berman-Frank, I., Bopp, L., Boyd, P. W., Galbraith, E. D., Geider, R. J., Guieu, C., Jaccard, S. L., Jickells, T. D., La Roche, J., Lenton, T. M., Mahowald, N. M., Maranon, E.,

https://doi.org/10.5194/egusphere-2025-4058
Preprint. Discussion started: 28 August 2025

Marinov, I., Moore, J. K., Nakatsuka, T., Oschlies, A., Saito, M. A., Thingstad, T. F., Tsuda, A., and Ulloa, O.: Processes and patterns of oceanic nutrient limitation, Nature Geoscience, 6, 701-710, 10.1038/ngeo1765, 2013.

Moreno, N., Querol, X., Andrés, J. M., Stanton, K., Towler, M., Nugteren, H., Janssen-Jurkovicová, M., and Jones, R.: Physico-chemical characteristics of European pulverized coal combustion fly ashes, Fuel, 84, 1351-1363, https://doi.org/10.1016/j.fuel.2004.06.038, 2005.

Myriokefalitakis, S., Ito, A., Kanakidou, M., Nenes, A., Krol, M. C., Mahowald, N. M., Scanza, R. A., Hamilton, D. S., Johnson, M. S., Meskhidze, N., Kok, J. F., Guieu, C., Baker, A. R., Jickells, T. D., Sarin, M. M., Bikkina, S., Shelley, R., Bowie, A., Perron, M. M. G., and Duce, R. A.: Reviews and syntheses: the GESAMP atmospheric iron deposition model intercomparison study, Biogeosciences, 15, 6659-6684, 10.5194/bg-15-6659-2018, 2018.

Nishioka, J., and Obata, H.: Dissolved iron distribution in the western and central subarctic Pacific: HNLC water formation and biogeochemical processes, Limnology and Oceanography, 62, 2004-2022, https://doi.org/10.1002/lno.10548, 2017.

Oakes, M., Ingall, E. D., Lai, B., Shafer, M. M., Hays, M. D., Liu, Z. G., Russell, A. G., and Weber, R. J.: Iron Solubility Related to Particle Sulfur Content in Source Emission and Ambient Fine Particles, Environmental Science & Technology, 46, 6637-6644, 10.1021/es300701c, 2012.

Oliveira, C. M., Machado, C. M., Duarte, G. W., and Peterson, M.: Beneficiation of pyrite from coal mining, Journal of Cleaner Production, 139, 821-827, https://doi.org/10.1016/j.jclepro.2016.08.124, 2016.

Ooki, A., Nishioka, J., Ono, T., and Noriki, S.: Size dependence of iron solubility of Asian mineral dust particles, Journal of Geophysical Research: Atmospheres, 114, 10.1029/2008JD010804, 2009.

Patil, R. S., Kumar, R., Menon, R., Shah, M. K., and Sethi, V.: Development of particulate matter speciation profiles for major sources in six cities in India, Atmospheric Research, 132-133, 1-11, https://doi.org/10.1016/j.atmosres.2013.04.012, 2013.

Perron, M. M. G., Fietz, S., Hamilton, D. S., Ito, A., Shelley, R. U., and Tang, M.: Preface to the inter-journal special issue "RUSTED: Reducing Uncertainty in Soluble aerosol Trace Element Deposition", Atmospheric Measurement Techniques, 17, 165-166, 10.5194/amt-17-165-2024, 2024.

Raclavská, H., Corsaro, A., Hartmann-Koval, S., and Juchelková, D.: Enrichment and distribution of 24 elements within the sub-sieve particle size distribution ranges of fly ash from wastes incinerator plants, Journal of Environmental Management, 203, 1169-1177, https://doi.org/10.1016/j.jenvman.2017.03.073, 2017.

Ram, L. C., Tripathi, P. S. M., and Mishra, S. P.: Mössbauer spectroscopic studies on the transformations of iron-bearing minerals during combustion of coals: Correlation with fouling and slagging, Fuel Processing Technology, 42, 47-60, https://doi.org/10.1016/0378-3820(94)00111-6, 1995.

Rathod, S. D., Hamilton, D. S., Mahowald, N. M., Klimont, Z., Corbett, J. J., and Bond, T. C.: A Mineralogy-Based Anthropogenic Combustion-Iron Emission Inventory, Journal of Geophysical Research: Atmospheres, 125, e2019JD032114, https://doi.org/10.1029/2019JD032114, 2020.

Rathod, S. D., Hamilton, D. S., Nino, L., Kreidenweis, S. M., Bian, Q., Mahowald, N. M., Alastuey, A., Querol, X., Paytan, A., Artaxo, P., Herut, B., Gaston, C., Prospero, J., Chellam, S., Hueglin, C., Varrica, D., Dongarra, G., Cohen, D. D., Smichowski, P., Gomez, D., Lambert, F., Barraza, F., Bergametti, G., Rodríguez, S., Gonzalez-Ramos, Y., Hand, J., Kyllönen, K., Hakola, H., Chuang, P., Hopke, P. K., Harrison, R. M., Martin, R. V., Walsh, B., Weagle, C., Maenhaut, W., Morera-Gómez, Y., Chen, Y.-C., Pierce, J. R., and Bond, T. C.: Constraining Present-Day Anthropogenic Total Iron Emissions Using Model and Observations, Journal of Geophysical Research: Atmospheres, 129, e2023JD040332, https://doi.org/10.1029/2023JD040332, 2024.

Riahi, K., van Vuuren, D. P., Kriegler, E., Edmonds, J., O'Neill, B. C., Fujimori, S., Bauer, N., Calvin, K., Dellink, R., Fricko, O., Lutz, W., Popp, A., Cuaresma, J. C., Kc, S., Leimbach, M., Jiang, L., Kram, T., Rao, S.,

https://doi.org/10.5194/egusphere-2025-4058
Preprint. Discussion started: 28 August 2025

Emmerling, J., Ebi, K., Hasegawa, T., Havlik, P., Humpenöder, F., Da Silva, L. A., Smith, S., Stehfest, E., Bosetti, V., Eom, J., Gernaat, D., Masui, T., Rogelj, J., Strefler, J., Drouet, L., Krey, V., Luderer, G., Harmsen, M., Takahashi, K., Baumstark, L., Doelman, J. C., Kainuma, M., Klimont, Z., Marangoni, G., Lotze-Campen, H., Obersteiner, M., Tabeau, A., and Tavoni, M.: The Shared Socioeconomic Pathways and their energy, land use, and greenhouse gas emissions implications: An overview, Global Environmental Change, 42, 153-168, https://doi.org/10.1016/j.gloenvcha.2016.05.009, 2017.

Scanza, R. A., Hamilton, D. S., Perez Garcia-Pando, C., Buck, C., Baker, A., and Mahowald, N. M.: Atmospheric processing of iron in mineral and combustion aerosols: development of an intermediate-complexity mechanism suitable for Earth system models, Atmospheric Chemistry and Physics, 18, 14175-14196, 10.5194/acp-18-14175-2018, 2018.

Schmidl, C., Marr, I. L., Caseiro, A., Kotianová, P., Berner, A., Bauer, H., Kasper-Giebl, A., and Puxbaum, H.: Chemical characterisation of fine particle emissions from wood stove combustion of common woods growing in mid-European Alpine regions, Atmospheric Environment, 42, 126-141, https://doi.org/10.1016/j.atmosenv.2007.09.028, 2008.

Schroth, A. W., Crusius, J., Sholkovitz, E. R., and Bostick, B. C.: Iron solubility driven by speciation in dust sources to the ocean, Nature Geoscience, 2, 337-340, 10.1038/ngeo501, 2009.

Shi, Z. B., Woodhouse, M. T., Carslaw, K. S., Krom, M. D., Mann, G. W., Baker, A. R., Savov, I., Fones, G. R., Brooks, B., Drake, N., Jickells, T. D., and Benning, L. G.: Minor effect of physical size sorting on iron solubility of transported mineral dust, Atmospheric Chemistry and Physics, 11, 8459-8469, 10.5194/acp-11-8459-2011, 2011.

Silva, V. S., Silva, J. S., Costa, B. d. S., Labes, C., and Oliveira, R. M. P. B.: Preparation of glaze using electric-arc furnace dust as raw material, Journal of Materials Research and Technology, 8, 5504-5514, https://doi.org/10.1016/j.jmrt.2019.09.018, 2019.

Sippula, O., Hokkinen, J., Puustinen, H., Yli-Pirilä, P., and Jokiniemi, J.: Comparison of particle emissions from small heavy fuel oil and wood-fired boilers, Atmospheric Environment, 43, 4855-4864, https://doi.org/10.1016/j.atmosenv.2009.07.022, 2009.

Sippula, O., Stengel, B., Sklorz, M., Streibel, T., Rabe, R., Orasche, J., Lintelmann, J., Michalke, B., Abbaszade, G., Radischat, C., Gröger, T., Schnelle-Kreis, J., Harndorf, H., and Zimmermann, R.: Particle Emissions from a Marine Engine: Chemical Composition and Aromatic Emission Profiles under Various Operating Conditions, Environmental Science & Technology, 48, 11721-11729, 10.1021/es502484z, 2014.

Souza, C. A. C. D., Machado, A. T., Lima, L. R. P. d. A., and Cardoso, R. J. C.: Stabilization of electric-arc furnace dust in concrete, Materials Research, 13, 513-519, https://doi.org/10.1590/S1516-14392010000400014, 2010.

Stathopoulos, V. N., Papandreou, A., Kanellopoulou, D., and Stournaras, C. J.: Structural ceramics containing electric arc furnace dust, J Hazard Mater, 262, 91-99, https://doi.org/10.1016/j.jhazmat.2013.08.028, 2013.

Stoner, O., Lewis, J., Martínez, I. L., Gumy, S., Economou, T., and Adair-Rohani, H.: Household cooking fuel estimates at global and country level for 1990 to 2030, Nature Communications, 12, 5793, 10.1038/s41467-021-26036-x, 2021.

Tagliabue, A., Aumont, O., and Bopp, L.: The impact of different external sources of iron on the global carbon cycle, Geophysical Research Letters, 41, 920-926, https://doi.org/10.1002/2013GL059059, 2014.

Tagliabue, A., Bowie, A. R., Boyd, P. W., Buck, K. N., Johnson, K. S., and Saito, M. A.: The integral role of iron in ocean biogeochemistry, Nature, 543, 51-59, 10.1038/nature21058, 2017.

Tang, M., Perron, M. M. G., Baker, A. R., Li, R., Bowie, A. R., Buck, C. S., Kumar, A., Shelley, R., Ussher, S. J., Clough, R., Meyerink, S., Panda, P. P., Townsend, A. T., and Wyatt, N.: Measurement of soluble aerosol trace elements: inter-laboratory comparison of eight leaching protocols, EGUsphere, 2025, 1-38,

https://doi.org/10.5194/egusphere-2025-4058
Preprint. Discussion started: 28 August 2025

10.5194/egusphere-2025-3274, 2025.

Taylor, S. R., and McLennan, S. M.: The geochemical evolution of the continental crust, Reviews of Geophysics, 33, 241-265, https://doi.org/10.1029/95RG00262, 1995.

Tegler, L. A., Sherry, A. M., Herckes, P., Romaniello, S. J., and Anbar, A. D.: Up in Smoke: Most Aerosolized Fe From Biomass Burning Does Not Derive From Foliage, Global Biogeochemical Cycles, 37, e2023GB007796, https://doi.org/10.1029/2023GB007796, 2023.

Turnock, S. T., Allen, R. J., Andrews, M., Bauer, S. E., Deushi, M., Emmons, L., Good, P., Horowitz, L., John, J. G., Michou, M., Nabat, P., Naik, V., Neubauer, D., O'Connor, F. M., Olivié, D., Oshima, N., Schulz, M., Sellar, A., Shim, S., Takemura, T., Tilmes, S., Tsigaridis, K., Wu, T., and Zhang, J.: Historical and future changes in air pollutants from CMIP6 models, Atmospheric Chemistry and Physics, 20, 14547-14579, 10.5194/acp-20-14547-2020, 2020.

van Marle, M. J. E., Kloster, S., Magi, B. I., Marlon, J. R., Daniau, A. L., Field, R. D., Arneth, A., Forrest, M., Hantson, S., Kehrwald, N. M., Knorr, W., Lasslop, G., Li, F., Mangeon, S., Yue, C., Kaiser, J. W., and van der Werf, G. R.: Historic global biomass burning emissions for CMIP6 (BB4CMIP) based on merging satellite observations with proxies and fire models (1750–2015), Geoscientific Model Development, 10, 3329-3357, 10.5194/gmd-10-3329-2017, 2017.

Vieira, C. M. F., Sanchez, R., Monteiro, S. N., Lalla, N., and Quaranta, N.: Recycling of electric arc furnace dust into red ceramic, Journal of Materials Research and Technology, 2, 88-92, https://doi.org/10.1016/j.jmrt.2012.09.001, 2013.

Wan, X., Wang, W., Ye, T., Guo, Y., and Gao, X.: A study on the chemical and mineralogical characterization of MSWI fly ash using a sequential extraction procedure, J Hazard Mater, 134, 197-201, https://doi.org/10.1016/j.jhazmat.2005.10.048, 2006.

Wang, R., Balkanski, Y., Boucher, O., Bopp, L., Chappell, A., Ciais, P., Hauglustaine, D., Peñuelas, J., and Tao, S.: Sources, transport and deposition of iron in the global atmosphere, Atmospheric Chemistry and Physics, 15, 6247-6270, 10.5194/acp-15-6247-2015, 2015.

Ward, C. R.: Analysis, origin and significance of mineral matter in coal: An updated review, International Journal of Coal Geology, 165, 1-27, https://doi.org/10.1016/j.coal.2016.07.014, 2016.

Watson, J. G., Chow, J. C., and Houck, J. E.: PM2.5 chemical source profiles for vehicle exhaust, vegetative burning, geological material, and coal burning in Northwestern Colorado during 1995, Chemosphere, 43, 1141-1151, https://doi.org/10.1016/S0045-6535(00)00171-5, 2001.

Wu, C., Lin, Z., and Liu, X.: The global dust cycle and uncertainty in CMIP5 (Coupled Model Intercomparison Project phase 5) models, Atmospheric Chemistry and Physics, 20, 10401-10425, 10.5194/acp-20-10401-2020, 2020.

Wu, D., Li, Q., Ding, X., Sun, J., Li, D., Fu, H., Teich, M., Ye, X., and Chen, J.: Primary Particulate Matter Emitted from Heavy Fuel and Diesel Oil Combustion in a Typical Container Ship: Characteristics and Toxicity, Environmental Science & Technology, 52, 12943-12951, 10.1021/acs.est.8b04471, 2018.

Wu, H.-Y., and Ting, Y.-P.: Metal extraction from municipal solid waste (MSW) incinerator fly ash—Chemical leaching and fungal bioleaching, Enzyme and Microbial Technology, 38, 839-847, https://doi.org/10.1016/j.enzmictec.2005.08.012, 2006.

Wu, K., Shi, H., Schutter, G. D., Guo, X., and Ye, G.: Preparation of alinite cement from municipal solid waste incineration fly ash, Cement and Concrete Composites, 34, 322-327, https://doi.org/10.1016/j.cemconcomp.2011.11.016, 2012.

Xia, D. K., and Picklesi, C. A.: Microwave caustic leaching of electric arc furnace dust, Minerals Engineering, 13, 79-94, https://doi.org/10.1016/S0892-6875(99)00151-X, 2000.

https://doi.org/10.5194/egusphere-2025-4058
Preprint. Discussion started: 28 August 2025

Ye, L., Peng, Z., Ye, Q., Wang, L., Augustine, R., Perez, M., Liu, Y., Liu, M., Tang, H., Rao, M., Li, G., and Jiang, T.: Toward environmentally friendly direct reduced iron production: A novel route of comprehensive utilization of blast furnace dust and electric arc furnace dust, Waste Management, 135, 389-396, https://doi.org/10.1016/j.wasman.2021.08.045, 2021.

Zhang, H., Zhao, Y., and Qi, J.: Utilization of municipal solid waste incineration (MSWI) fly ash in ceramic brick: Product characterization and environmental toxicity, Waste Management, 31, 331-341, https://doi.org/10.1016/j.wasman.2010.10.017, 2011.

Zhang, H., Wang, S., Hao, J., Wan, L., Jiang, J., Zhang, M., Mestl, H. E. S., Alnes, L. W. H., Aunan, K., and Mellouki, A. W.: Chemical and size characterization of particles emitted from the burning of coal and wood in rural households in Guizhou, China, Atmospheric Environment, 51, 94-99, https://doi.org/10.1016/j.atmosenv.2012.01.042, 2012.

Zhang, H., Li, R., Dong, S., Wang, F., Zhu, Y., Meng, H., Huang, C., Ren, Y., Wang, X., Hu, X., Li, T., Peng, C., Zhang, G., Xue, L., Wang, X., and Tang, M.: Abundance and Fractional Solubility of Aerosol Iron During Winter at a Coastal City in Northern China: Similarities and Contrasts Between Fine and Coarse Particles, Journal of Geophysical Research: Atmospheres, 127, e2021JD036070, https://doi.org/10.1029/2021JD036070, 2022.